www.sciencemag.org/cgi/content/full/science.1220757/DC1

# Supplementary Materials for

## A *Papaver somniferum* 10-Gene Cluster for Synthesis of the Anticancer Alkaloid Noscapine

Thilo Winzer, Valeria Gazda, Zhesi He, Filip Kaminski, Marcelo Kern, Tony R. Larson, Yi Li, Fergus Meade, Roxana Teodor, Fabián E. Vaistij, Carol Walker, Tim A. Bowser, Ian A. Graham*

*To whom correspondence should be addressed. E-mail: ian.graham@york.ac.uk

Published 31 May 2012 on *Science* Express
DOI: 10.1126/science.1220757

**This PDF file includes:**



**Other Supplementary Material for this manuscript includes the following:**

Tables S5, S6, S8, and S9

## Materials and Methods

**Plant Material** Three GSK Australia poppy varieties that predominantly accumulate either noscapine (High Noscapine, HN1), morphine (High Morphine, HM1) or thebaine (High Thebaine HT1), were grown in Maxi (Fleet) Rootrainers$^{TM}$ (Haxnicks, Mere, UK) under glass in 16 hour days at the University of York horticulture facilities. The growth substrate consisted of 4 parts John Innes No. 2, 1 part Perlite and 2 parts Vermiculite.

The HM1×HN1 F2 mapping population was grown at the GlaxoSmithKline Australia field-trial site, Latrobe, Tasmania from September 2009 to February 2010.

**Crossing and selfing** Crosses were carried out between HN1and HM1 individuals to generate F1 hybrid seed. At the hook stage of inflorescence development, immature stamens were removed from selected HN1 flower buds. HN1 stigmas were fertilized with pollen from synchronously developing HM1 flowers shortly after onset of anthesis. To prevent contaminating

pollen from reaching the receptive stigmas, emasculated flowers were covered with a muslin bag for four days after pollination. Both the F1 and F2 generations were self-pollinated to produce F2 and F3 seed, respectively. Self-pollination was ensured by covering the flowers shortly before onset of anthesis with a muslin bag.

**RNA isolation and cDNA synthesis** Upper stems (defined as the 2 cm section immediately underneath the capsule) and whole capsules were harvested at two developmental stages represented by 1-3 days and 4-6 days, after petal fall. Five plants were used per developmental stage and cultivar. The material was ground to a fine powder in liquid nitrogen using a mortar and pestle. RNA was isolated from the powder using a CTAB-based extraction method (*33*) with small modifications: (i) three sequential extractions with chloroform:isoamylalcohol (24:1) were performed and (ii) the RNA was precipitated overnight with lithium chloride at 4°C. After spectrophotometric quantification, equal amounts of RNA were pooled from five plants per cultivar, development stage and organ. The pooled samples underwent a final purification step using an RNeasy Plus MicroKit (Qiagen, Crawley, UK). RNA was typically eluted in 30-100 µl water. cDNA was prepared with the SMART cDNA Library Construction Kit (Clontech, Saint-Germainen-Laye, France) according to the manufacturer's instructions but using SuperScript II Reverse Transcriptase (Invitrogen, Paisley, UK ) for first strand synthesis. The CDSIII/3'PCR primer was modified to: 5' ATT CTA GAT CCR ACA TGT TTT TTT TTT TTT TTT TTT TVN 3' where R = A or G, V = A, C or G; N = A/T or C/G. Following digestion with MmeI (New England Biolabs, Hitchin, UK) the cDNA was finally purified using a QIAquick PCR Purification kit (Qiagen, Crawley, UK).

**cDNA Pyrosequencing** Pyrosequencing was performed on the Roche 454 GS-FLX sequencing platform (Branford, CT) using cDNA prepared from the following four samples of each of the three varieties:

i. upper stem, 1-3 days after petal fall
ii. upper stem, 4 -6 days after petal fall
iii. capsule, 1-3 days after petal fall
iv. capsule, 4 -6 days after petal fall

**Raw sequence analysis, contiguous sequence assembly and annotation** The raw sequence datasets were derived from parallel tagged sequencing on the 454 sequencing platform (*34*). Primer and tag sequences were first removed from all individual sequence reads. Contiguous sequence assembly was only performed on sequences longer than 40 nucleotides and containing less than 3% unknown (N) residues. Those high quality Expressed Sequence Tag (EST) sequences were assembled into unique contiguous sequences with the CAP3 Sequence Assembly Program (*35*), and the resulting contigs were annotated locally using the BLAST2 program (*36*) against the non-redundant peptide database downloaded from the NCBI.

**Expression profiling** The number of ESTs associated with a specific consensus sequence representing each of the candidate genes detailed in Figure 1 was counted for each EST library. EST numbers were normalised on the basis of total number of ESTs obtained per library. For each variety, EST counts were combined for the two developmental stages from both stems and capsules. Differences in candidate gene expression levels between organs and varieties were visualised as a heat map using Microsoft Excel.

**Preparation of genomic DNA from glasshouse grown plants** In order to amplify and obtain genomic sequences of the candidate genes 30-50 mgs of leaf material was collected from 4-6 week old glasshouse-grown seedlings from each of the three varieties. Genomic DNA was extracted using the BioSprint 96 Plant kit on the BioSprint 96 Workstation (Qiagen, Crawley, UK) according to the manufacturer's protocol. Extracted DNA was quantified using Hoescht 33258 and normalized to 10 ng/ul.

**Amplification and sequencing of candidate genes from genomic DNA** Primers for amplification and Sanger-sequencing of the candidate genes from genomic DNA were based on the respective contiguous sequences assembled from the ESTs or on BAC sequences. The primer sequences are shown in Table S8. PCR amplifications were performed on pools of genomic DNA comprising DNA from four individuals. Amplification was typically carried out on 10 ng genomic DNA in 1× Phusion High Fidelity Buffer supplemented with 200 nM forward and reverse primers, 0.2 mM dNTPs, 0.02 units/µl Phusion Hot Start DNA Polymerase (Finnzymes, Vantaa, Finnland). Standard PCR conditions were used throughout with annealing temperatures and times dependent on primers and PCR equipment. The sequences of ten genes from the cluster have been submitted to the GenBank of the National Centre for Biotechnology Information (www.ncbi.nlm.nih.gov/genbank/) and are available under the accession numbers JQ658999 (*PSMT1*), JQ659000 (*PSMT2*), JQ659001 (*PSMT3*), JQ659002 (*CYP82X1*), Q659004 (*CYP82X2*), JQ659005 (*CYP82Y1*), JQ659003 (*CYP719A21*), JQ659006 (*PSCXE1*), JQ659007 (*PSSDR1*), and JQ659008 (*PSAT1*).

**DNA extraction from the field-grown F2 mapping population** 40-50 mg of leaf tissue was harvested from F2 plants at the 'small rosette' growth stage (~10 leaves present on each plant)

into 1.2 ml sample tubes. A 3 mm tungsten carbide bead was added to each tube and samples were kept at -80°C for a minimum of two hours prior to freeze-drying for 18 hours. Following freeze drying, samples were powdered by bead-milling (Model TissueLyser, Qiagen, Hilden, Germany) at 30 Hz for two 60 s cycles separated by plate inversion. DNA extraction was performed with the Nucleospin Plant II kit (Macherey-Nagel, Düren, Germany) using the supplied Buffer Set PL2/3 following the manufacturer's protocol for centrifugal extraction. DNA was quantified by UV- spectroscopy.

**Genotyping of the HN1×HM1 F2 mapping population for the presence or absence of the HN1-specific candidate genes** Plants of the F2 mapping population were genotyped for the presence or absence of eight candidate genes. The gene primer pairs (Table S8) were designed with fluorescent tags (5'-VIC®-labeled) for use on the ABI 3730xl capillary apparatus (Applied Biosystems, Foster City, CA). PCR amplifications were typically carried out on 10 ng genomic DNA in 1x GoTaq buffer supplemented with 1 mM $MgCl_2$, 500 nM forward and reverse primer, 0.125 mM dNTPs, 0.1 U GoTaq (Promega, Southampton, UK). The amplification conditions were: 1 min 94°C, 30-36 cycles of 30 s denaturation at 94°C, 30 s annealing at 62°C and 20-50 s extension at 72°C, followed by a final extension for 5 min at 72°C. Cycle number and extension times depended on the candidate gene (Table S8). Amplification products were diluted 1:20 in $H_2O$ and fractionated on an ABI 3730xl capillary sequencer (Applied Biosystems, Foster City, CA). Data were scored using GeneMarker™ software (Softgenetics, State College, PA).

**Poppy straw analysis from field grown F2 plants** Poppy capsules were harvested by hand from the mapping population once capsules had dried to approximately 10% moisture on the plant. After manually separating the seed from the capsule, the capsule straw samples (Poppy

Straw) were then ground in a ball mill (Model MM04, Retsch, Haan, Germany) into a fine powder. Samples of ground poppy straw were then weighed accurately to 2 ± 0.003 g and extracted in 50 ml of a 10% acetic acid solution. The extraction suspension was shaken on an orbital shaker at 200 rpm for a minimum of 10 min, then filtered to provide a clear filtrate. The final filtrate was passed through a 0.22 µm filter prior to analysis. The loss on drying (LOD) of the straw was determined by drying in an oven at 105°C for 3 hours.

All solutions were analysed using a Waters Acquity UPLC system (Waters Ltd., Elstree, UK). fitted with a Waters Acquity BEH C18 column, 2.1 mm × 100 mm with 1.7 micron packing. The mobile phase used a gradient profile with eluent A consisting of 10 mM ammonium bicarbonate of pH 10.2 and eluent B methanol. The mobile phase gradient conditions used are as listed in the table below with a linear gradient. The flow rate was 0.5 ml per minute and the column maintained at 60°C. The injection volume was 2 µl and eluted peaks were ionised in positive APCI mode and detected within 5 ppm mass accuracy using a Thermo LTQ-Orbitrap. The runs were controlled by Thermo Xcalibur software (Thermo Fisher Scientific Inc., Hemel Hempstead, UK).

– Gradient Flow Program:

| **TIME (minutes)** | **% Eluent A** | **% Eluent B** | **Flow (ml/min)** |
|---|---|---|---|
| 0.0 | 98. | 2.0 | 0.50 |
| 0.2 | 98.0 | 2.0 | 0.50 |
| 0.5 | 60.0 | 40 | 0.50 |
| 4.0 | 20.0 | 80.0 | 0.50 |
| 4.5 | 20.0 | 80.0 | 0.50 |

Mass spectra were collected over the 150-900 m/z range at a resolution setting of 7500. All data analysis was carried out in the R programming language in a 64-bit Linux environment (R 2.11). Peak-picking was performed using the Bioconductor package, XCMS (*37*), employing the centWave algorithm (*38*). Redundancy in peak lists was reduced using the CAMERA package (*39*). Alkaloids were identified by comparing exact mass and retention time values to those of standards and quantified by their pseudomolecular ion areas using custom R scripts.

**Bacterial Artificial Chromosome (BAC) library construction** The HN1 BAC library was constructed from high molecular weight (HMW) genomic DNA processed at Amplicon Express, Inc. ( Pullman, WA) from four week old seedlings using the method described (*40*). The HMW DNA was partially digested with the restriction enzyme HindIII and size selected prior to ligation of fragments into the pCC1BAC vector (Epicentre Biotechnologies, Madison, WI) and transformation of DH10B *E. coli* cells, which were then plated on Luria-Bertani (LB) agar with chloramphenicol, X-gal and IPTG at appropriate concentrations. Clones were robotically picked with a Genetix QPIX (Molecular Devices, Sunnyvale, CA) into 240 384-well plates containing LB freezing media. Plates were incubated for 16 hours, replicated and then frozen at -80°C. The replicated copy was used as a source plate for nylon filters that were made and used for screening using the PCR DIG Probe Synthesis Kit (Roche Applied Science, Indianapolis, IN). To estimate insert sizes, DNA aliquots of 10 BAC minipreps were digested with 5U of NotI enzyme for 3 hours at 37°C. The digestion products were separated by pulsed-field gel electrophoresis (CHEF-DRIII system, Bio-Rad, Hercules, CA) in a 1% agarose gel in TBE. Insert sizes were compared to those of the Lambda Ladder MidRange I PFG Marker (New England Biolabs, Ipswich, MA). Electrophoresis was carried out for 18 hours at 14°C with an initial switch time

of 5 s, a final switch time of 15 s, in a voltage gradient of 6 V/cm. The average BAC clone size for the library was found to be 150 Kb.

**Filter construction and screening** Filter design and screening was carried out at Amplicon Express, Inc. (Pullman, WA). Bioassay dishes containing LB agar plate media and 12.5 µg/mL chloramphenicol were prepared. Positively charged nylon Amersham Hybond-$N^+$ membrane (GE Healthcare Bio-Sciences, Piscataway, NJ) was applied to the media surface and the GeneMachines G3 (Genomics Solutions, Bath, UK) was used to robotically grid 18,432 clones in duplicate on filters. The filters were incubated at 37˚C for 12 to 14 hours. The filters were processed using the nylon filter lysis method (*41*) with slight modifications. Following processing, the DNA was linked to the hybridization membrane filters according to the Hybond N+ manual by baking at 80°C for 2 hours. To screen the library a 643 bp digoxigenin (DIG)-labeled probe representing position 2161–2803 in the genomic sequence of *CYP82X2* (GenBank accession JQ659004) was generated from 1.5 ng gDNA by PCR reaction using the primers shown in Table S8 and the PCR DIG synthesis kit (Roche Applied Science, Indianapolis, IN) according to the manufacturer's instructions. A non-labeled probe was amplified, diluted and spotted to each filter in the following dilutions of 2 ng, 1 ng, 0.1 ng and 0.0 ng as a positive control. The controls were baked at 80°C for 30 min. Following a 30 min prehybridizing wash in DIG EasyHyb solution at 45°C approximately 0.5 µl of denatured DIG labeled PCR product was added per ml of hybridization solution with the nylon filters and incubated with gentle shaking overnight at 45°C. The nylon filters were washed twice in a 2× standard sodium citrate (SSC), 0.1% sodium dodecyl sulfate (SDS) buffer at room temperature for 5 min each, and twice with a 0.5× SSC, 0.1% SDS buffer at 65°C for 15 minutes each. The hybridized probe was detected

using NBT/BCIP stock solution according to the manufacturer's instructions (Roche Applied Science, Indianapolis, IN) and was found to hybridize to six BAC clones.

**BAC sequencing and automated sequence assembly** The six positive BAC clones from the BAC library were sequenced at Amplicon Express, Inc. (Pullman, WA) by Focused Genome Sequencing (FGS) with an average depth of 100× coverage. FGS is a Next Generation Sequencing (NGS) method developed at Amplicon Express that allows very high quality assembly of BAC clone sequence data using the Illumina HiSeq platform (Illumina,Inc, San Diego, CA). The proprietary FGS process makes NGS tagged libraries of BAC clones and generates a consensus sequence of the BAC clones with all reads assembled at 80 bp overlap and 98% identity. The gapped contiguous sequences were ordered and orientated manually based on mate pair sequences from four libraries of insert size 5000, 2000, 500 and 170 bp. Overlapping BAC clones, PS_BAC193L09, PS_BAC179L19, PS_BAC150A23 and PS_BAC164F07, which together encoded all 10 genes from the HN1 cluster, were selected for further sequence assembly (Table S5). Where possible, gaps and ambiguous regions on both BAC clones were covered by primer walking with traditional Sanger sequencing to validate the assembly. Combination of the four overlapping BAC sequences gave a single continuous consensus sequence assembly of 401 Kb. The sequences of the 10 genes from the HN1 cluster were determined independently by Sanger sequencing and the 100% agreement of the Sanger determined gene sequences with the assembly from FGS provided quality assurance for the whole assembly. The sequences of the BAC clones PS_BAC193L09, PS_BAC179L19, PS_BAC150A23 and PS_BAC164F07 have been submitted to the GenBank of the National Centre for Biotechnology Information

(www.ncbi.nlm.nih.gov/genbank/) and are available under the accession numbers JQ659010, JQ659009, JQ659011 and JQ659012, respectively.

**Annotation of the assembled sequence** The sequences of the four BAC clones were annotated with an automated gene prediction program FGENESH (*42*). The gene structure including exon-intron arrangement for the 10 genes in the HN1 cluster was validated by comparison with cDNA sequence for each gene (Table S5). cDNA sequence was not available for any of the remaining ORFs detailed in Table S5 since they are not represented in any of our EST libraries. The predicted function of all ORFs was evaluated by BLAST analysis (*36*) and those ORFs with significant hits (e-value less than $1e^{-8}$) were included in Fig.3. The assembled sequence of the whole 401 Kb HN1 gene cluster region was analyzed for repetitive/transposon content using the Repeatmasker program at http://repeatmasker.org .

**Promoter region analysis** The 1 Kb of DNA sequence upstream of the predicted start of translation for each of the 10 genes in the HN1 cluster were searched for the presence of plant *cis*-acting DNA elements using the PLACE database (*20*). The results are shown in Table S6.

**Amino acid sequence alignment** Multiple amino acid sequence alignment was performed using the ClustalW program (*43*) for each of the 10 genes in the HN1 cluster. The amino acid sequence encoded by each gene was compared against either the top hits from a BLAST search of the NCBI non-redundant protein database (*36*) or the protein sequences of functionally characterized homologues. In those cases were the predicted protein sequence for the 10 genes showed high similarity a combined ClustalW analysis was performed, for example in the case of PSMT2 and PSMT3.

**Generation of plasmid constructs for Virus Induced Gene Silencing (VIGS)** The tobacco rattle virus (TRV) based gene silencing system (*44*) was used to investigate the gene function of *PSMT1, PSMT2, CYP719A21, CYP82X2, PSSDR1* and *PSCXE1*. DNA fragments selected for silencing were amplified by PCR and cloned into the silencing vector pTRV2 (GenBank accession AF406991). They were linked to a 129 bp-long fragment of the *P. somniferum PHYTOENE DESATURASE* gene (*PSPDS*) in order to simultaneously silence the respective candidate genes and *PSPDS*. Plants displaying the photo-bleaching phenotype resulting from *PSPDS* silencing (*23*) were identified as plants successfully infected with the respective silencing constructs and selected for further analysis.

Generation of the pTRV2:PDS construct: A 622 bp fragment of *PSPDS* was amplified from cDNA prepared from HN1 using primers shown in Table S8. Its sequence has been submitted to GenBank and is available under the accession number JQ659013. Sau3AI digestion of the 622 bp PCR product yielded among others a fragment of 129 bp (corresponding to position 442-570 within JQ659013), which was cloned into the BamHI site of the pTRV2 vector. The orientation and fidelity was confirmed by sequencing and the resulting pTRV2:PDS vector was used in the generation of the VIGS construct for each candidate gene. The pTRV2:PDS construct also served as the control in the VIGS experiments.

DNA fragments selected for silencing the respective candidate genes were amplified from either HN1 genomic or cDNA. Primers used for amplification as well as the positions of the selected sequences within the respective open reading frames are shown in Table S8. The *PSMT1, CYP719A21* and *CYP82X2* fragments were first cloned into pTV00 (*45*) using HindIII and KpnI and then subcloned into pTRV2:PDS using BamHI and KpnI. *PSMT2, PSCXE1* and *PSSDR1*

fragments were cloned directly into pTRV2:PDS using BamHI and KpnI. The orientation and fidelity of all constructs was confirmed by sequencing.

**Transformation of *Agrobacterium tumefaciens* with VIGS constructs** VIGS constructs were propagated in *E. coli* strain DH5α and transformed into electrocompetent *Agrobacterium tumefaciens* (strain GV3101) by electroporation.

**Infiltration of plants** Separate overnight liquid cultures of *A. tumefaciens* containing individual VIGS constructs (each consisting of a selected DNA fragment from the target gene linked to a 129 bp-long fragment from the *P. somniferum PHYTOENE DESATURASE* gene) were used to inoculate LB medium containing 10 mM MES, 20 μM acetosyringone and 50μg/ml kanamycin. Cultures were maintained at 28°C for 24 hours, harvested by centrifugation at 3000×g for 20 min, and resuspended in infiltration solution (10 mM MES, 200 μM acetosyringone, 10 mM $MgCl_2$,) to an $OD_{600}$ of 2.5. *A. tumefaciens* harbouring the individual VIGS constructs including the control, pTRV2:PDS, were each mixed 1:1 (v/v) with *A. tumefaciens* containing pTRV1 (GenBank accession AF406990), and incubated for two hours at 22°C prior to infiltration. Two week old seedlings of HN1 grown under standard greenhouse conditions (22°C, 16h photoperiod), with emerging first leaves, were infiltrated as described (*16*).

**Gene Expression analysis of F1 and VIGS plants** For gene expression analysis in the F1, 5 cm long shoot fragments were harvested from the distal end (underneath the flower bud) of 8-9 week old F1: HM1×HN1 plants and the parental lines, HM1 and HN1. For gene expression analysis in VIGS plants, the youngest leaves of 7 week old infiltrated plants (developmentally staged as first

emerging flower buds) displaying photo-bleaching were harvested for RNA isolation. Total RNA was isolated using silica-membrane columns (RNeasy Plant Mini Kit, Qiagen, Crawley, UK) according to the manufacturer's instructions. Reverse transcription was performed at 42°C for 50 min, using oligo$(dT)_{12\text{-}18}$ primer, 1µg RNA, and SuperScriptII reverse transcriptase in 12 µl volume, according to the manufacturer's instructions (Invitrogen, Paisley, UK). Following the reverse transcription, the RNA-primer mix was denatured at 70°C for 5 min. Quantitative real-time PCR (qPCR) was performed with SYBR Green, using the MyIQ Single Color Real-Time PCR Detection system (Bio-Rad, Hemel Hempstead, UK). Each 20-µl PCR included 6.8 µl of cDNA (taken from a 1:9 v/v dilution of the RT reaction with molecular grade water), 1.6 µl each of the forward and reverse primers (10 µM), and 2× Power SYBR Green PCR Master Mix (Life Technologies, Carlsbad, CA). Primer sequences are listed in Table S8. Reactions were subjected to 40 cycles of template denaturation, primer annealing and primer extension. To evaluate qPCR specificity, the amplicons of all primer pairs were subjected to a melting-curve analysis using the dissociation method suggested by the instrument manufacturer. Gene expression data were determined based on 9 independent values per plant line or VIGS construct, respectively (i.e. 3 technical replicates of 3 individual plants). The $2^{-\Delta\Delta Ct}$ method was used for the analysis of relative gene expression (*46*). The expression of actin served as an internal control for normalisation. Expression levels of *PSMT1* and *PSMT2* in HM1 and F1: HM1×HN1 plants were compared to those in HN1 plants. Levels of gene expression in HN1 were used as the calibrator for each gene. Expression levels of the candidate genes in plants infected with their respective VIGS constructs were compared to those in plants silenced only for *PSPDS* as a control. The plant line showing the highest expression level served as the calibrator for each target gene.

**Latex and capsule analysis of silenced plants** Leaf latex of infiltrated plants displaying photo-bleaching as a visual marker for successful infection and silencing was analyzed when the first flower buds emerged (~7 week old plants). Latex was collected from cut petioles, with a single drop dispersed into 500 µl of 10% acetic acid. This was diluted 10× in 1% acetic acid to give an alkaloid solution in 2% acetic acid for further analysis. Capsules were harvested from the same plants used for latex analysis and single capsules were ground to a fine powder in a ball mill (Model MM04, Retsch, Haan, Germany). Samples of ground poppy straw were then weighed accurately to 10 ± 0.1 mg and extracted in 0.5 ml of a 10% acetic acid solution with gentle shaking for 1h at room temperature. Samples were then clarified by centrifugation and a 50 µl subsample diluted 10× in 1% acetic acid to give an alkaloid solution in 2% acetic acid for further analysis. All solutions were analyzed as described for the poppy straw analysis from field grown F2 plants. Likewise, all data analysis was carried out using the R programming language. Putative alkaloid peaks were quantified by their pseudomolecular ion areas using custom scripts. Peak lists were compiled and any peak-wise significant differences between samples were identified using 1-way ANOVA with p-values adjusted using the Bonferroni correction for the number of unique peaks in the data set. For any peak-wise comparisons with adjusted p-values < 0.05, Tukey's HSD test was used to identify peaks that were significantly different between any given sample and the control. Alkaloids were identified by comparing exact mass and retention time values to those of standards. Where standards were not available, the Bioconductor rcdk package (*37*) was used to generate pseudomolecular formulae from exact masses within elemental constraints C = 1 100, H = 1 200, O = 0 200, N = 0 3 and mass accuracy < 5ppm. The hit with the lowest ppm error within these constraints was used to assign a putative formula.

**Cloning and heterologous expression of *PSMT1* in *Saccharomyces cerevisiae***

Cloning and protein production in *S. cerevisiae* were performed using the pESC Yeast Epitope Tagging System (Agilent Technologies, USA). The full-length coding sequence of *PSMT1* was amplified from cDNA obtained from mRNA extracted from the HN1 variety using primers described in Table S8. These primers introduced *Bam*HI (forward primer) and *Xho*I sites (reverse primer) and the resulting PCR product was directionally cloned using the *Bam*HI and *Xho*I sites of the pESC-TRP vector (Agilent Technologies, USA). The resulting pESC-TRP:PSMT1 construct was transformed into *E. coli* strain DH5α. Fidelity of the insert was confirmed by DNA sequencing.

**Yeast transformation and protein production**

pESC-TRP:PSMT1 was transformed into *Saccharomyces cerevisiae* strain G175 using the lithium acetate method following the protocol described by the manufacturer (Agilent Technologies, USA). Briefly, G175 strain was grown overnight in 50 mL YAPD broth (0.0075% (w/v) *L*-adenine hemisulfate salt, 1% (w/v) yeast extract, 2% (w/v) peptone, 2% (w/v) glucose and diluted to an $OD_{600}$ = 0.25 in fresh YPAD broth and incubated at 30°C until $OD_{600}$ = 1.0. Cells were harvested and resuspended in 10 mL LTE buffer (100 mM LiOAc, 10 mM Tris-HCl pH 7.5, 1 mM EDTA), spun at 3,000 rpm for 5 min and resuspended in 0.5 mL LTE buffer. 50 µL of this cell suspension was then used for each transformation, carried out by mixing 1 µg of pESC-TRP:PSMT1, 300 µL transformation mix (40% (w/v) PEG 3350, 100 mM LiOAc, 10 mM Tris-HCl pH 7.5, 1 mM EDTA) followed by a 30 min incubation at 30°C and a 15 min incubation at 42°C. Transformants were selected on synthetic medium plates containing glucose (0.67% (w/v) yeast nitrogen base without amino acids, 2% (w/v) glucose, 0.13% (w/v) amino acid drop out mix not containing tryptophan, 2% (w/v) Bacto Agar) after a 3-day incubation at 30°C. Colonies were then streaked out on fresh selective medium and tested for the presence of insert. One yeast colony was resuspended in 50µL 10 mM Tris-Cl pH 7.5, 1 mM EDTA, Lyticase 100-50 U/µL and incubated for 30 min at 37°C and then 10 min at 95°C. The suspension was clarified by spinning the products for 5 min at 13,000 rpm on a benchtop microfuge. PSMT1 insert was checked by PCR using vector primers Gal1 FOR 5'ATT TTC GGT TTG TAT TAC TTC-3' and Gal1 Rev 5'-GTT CTT AAT ACT AAC ATA ACT-3' following the cycling conditions described by the manufacturer.

Recombinant protein production was carried out following described methods (*47*) with the following modifications. Selected transformants carrying the PSMT1 insert were inoculated in 10 mL synthetic broth containing glucose and grown overnight at 30°C in shake flasks. Cells were harvested by centrifugation of cultures at 3,000 rpm on a benchtop centrifuge for 5 min and washed twice in sterile 0.9% (w/v) NaCl. Cell pellets were resuspended in 5 mL synthetic broth containing raffinose and galactose (0.67% (w/v) yeast nitrogen base without amino acids, 2% (w/v) galactose, 1.5% (w/v) raffinose, 0.13% (w/v) amino acid drop out mix not containing tryptophan) and incubated at 30°C for 6 h at 200 rpm to induce the expression of recombinant PSMT1. Sterile scoulerine HCl (APIN Chemicals Ltd, Oxon, UK) prepared in 100 mM Acetate buffer pH4.5 was added to the cultures to a final concentration of 15 μM. After 3 days, cultures were harvested by centrifugation and a 2μL aliquot of supernatant analysed by UPLC-MS.

## Supplementary Figures

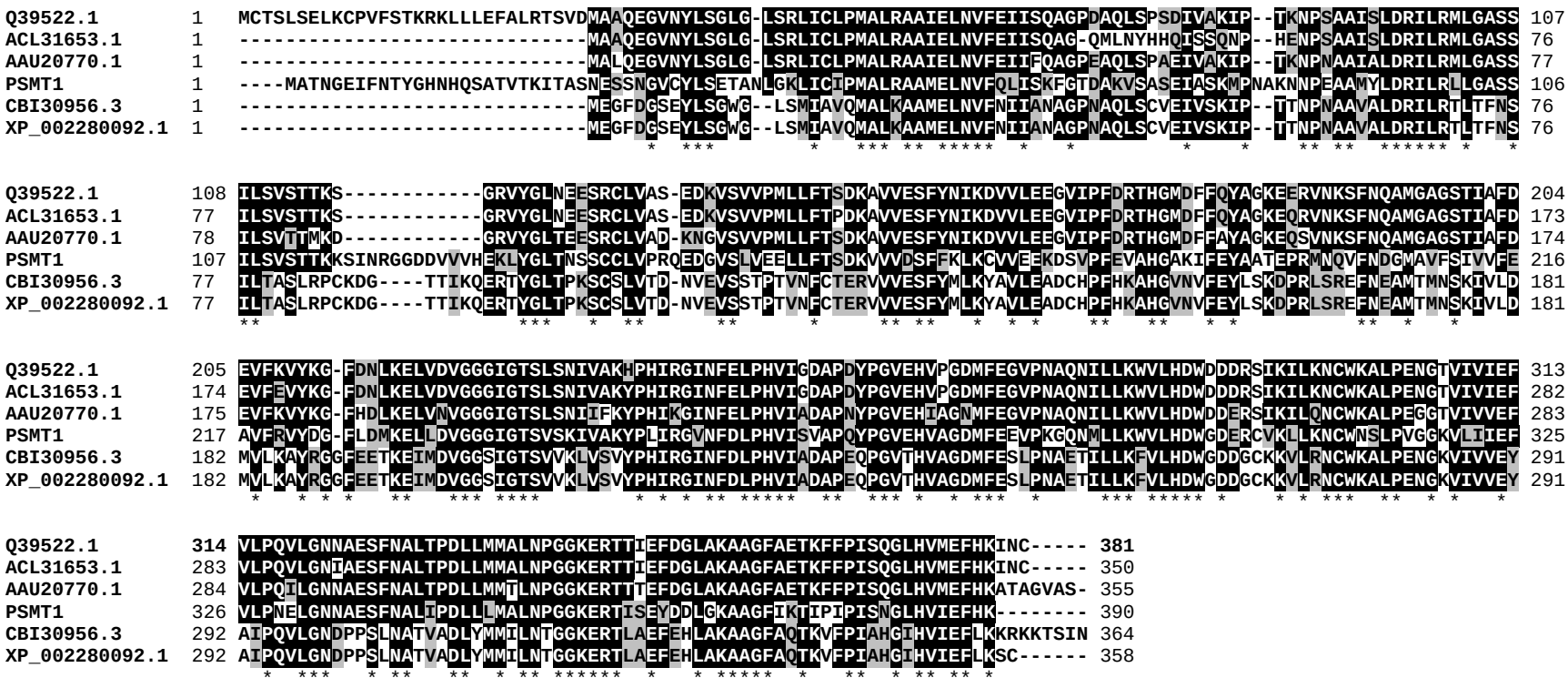


**Fig. S1a. Sequence alignment of the deduced amino acid sequence of PSMT1 with the five top hits from a BLAST search of the NCBI non-redundant protein database (S4).** PSMT1 shows high homology to the functionally characterized scoulerine 9-*O*-methyltransferase from *Coptis japonica*. Sequences were aligned in Clustal W (*43*). Residues identical in at least 50% of the sequences are shaded in black, similar residues in grey. An * (asterisk) underneath the alignment indicates positions which have a single, fully conserved residue. Q39522.1, *Coptis japonica* (S)-scoulerine 9-*O*-methyltransferase; ACL31653.1, *Coptis chinensis* (S)-scoulerine 9-*O*-methyltransferase; AAU20770.1, *Thalictrum flavum* scoulerine 9-*O*-methyltransferase; CBI30956.3, *Vitis vinifera* unnamed protein product; CBI30956.3, *Vitis vinifera* predicted (S)-scoulerine 9-O-methyltransferase.


**Fig. S1b. Sequence alignment of the deduced amino acid sequence of PSMT2 and PSMT3 with the combined five top hits from a BLAST search of the NCBI non-redundant protein database (S4).** PSMT2 and PSMT3 show homology to *O*-methyltransferases involved in benzylisoquinoline alkaloid biosynthesis. Sequences were aligned in Clustal W (*43*). Residues identical in at least 50% of the sequences are shaded in black, similar residues in grey. An * (asterisk) underneath the alignment indicates positions which have a single, fully conserved residue. AAP45315.1, *Papaver somniferum* S-adenosyl-L-methionine:norcoclaurine 6-O-methyltransferase; AAQ01669.1, *Papaver somniferum* (R,S)-norcoclaurine 6-O-methyltransferase; ACO90232.1, *Papaver bracteatum* putative norcoclaurine 6-O-methyltransferase; ACO90225.1, *Papaver bracteatum* putative norcoclaurine 6-O-methyltransferase; ACN88562.1, *Papaver somniferum* norreticuline-7-O-methyltransferase;

Q9LEL6.1, *Coptis japonica* (R,S)-norcoclaurine 6-O-methyltransferase; AAP45314.1, *Papaver somniferum* S-adenosyl-L-methionine:3'-hydroxy-N-methylcoclaurine 4'-O-methyltransferase 2.

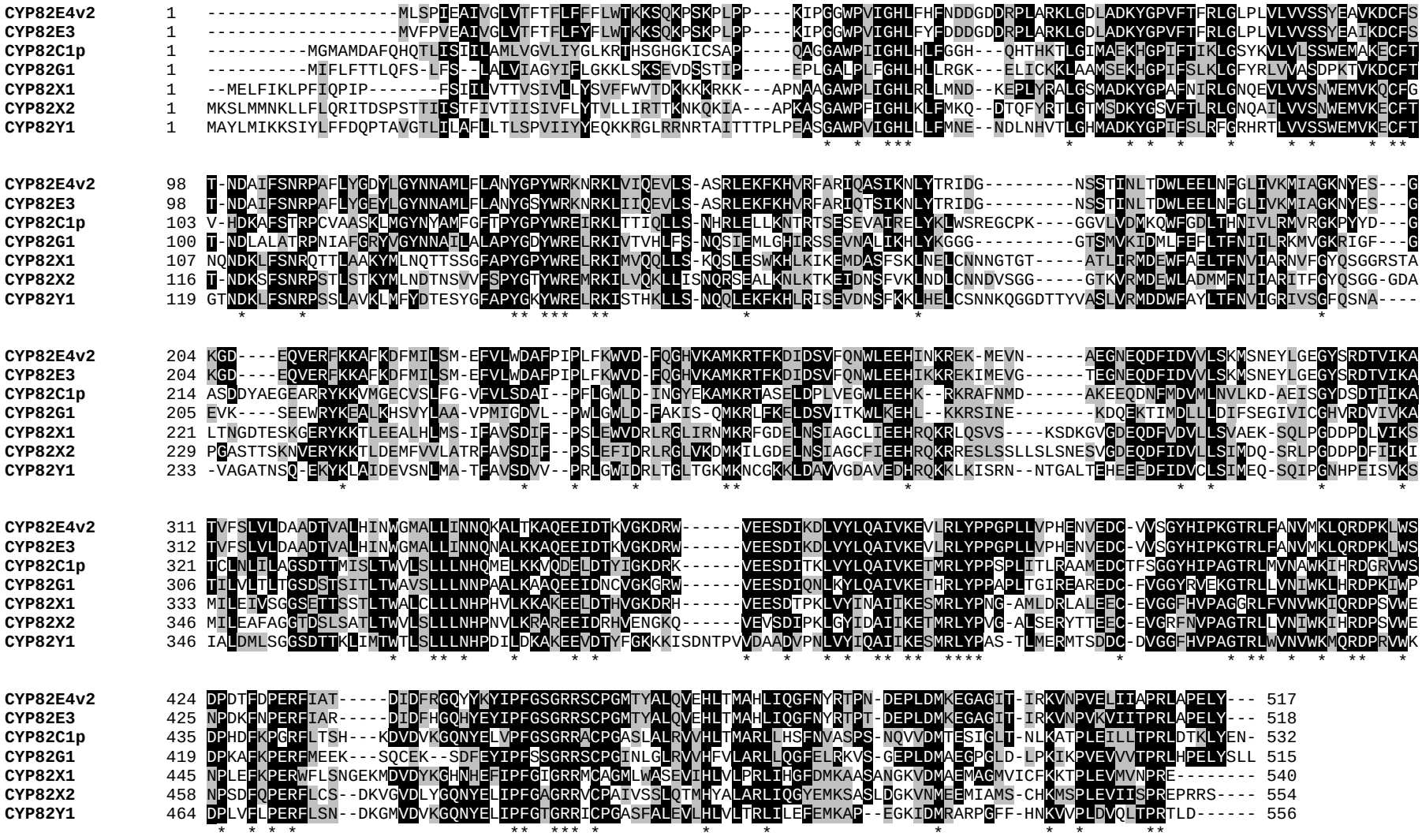


**Fig. S2a. Sequence alignment of the deduced amino acid sequence of CYP82X1, CYP82X2 and CYP82Y1 with functionally characterized members of the CYP82 family of cytochrome P450 oxygenases.** Sequences were aligned in Clustal W (*43*). Residues identical in at least 50% of the sequences are shaded in black, similar residues in grey. An * (asterisk) underneath the alignment indicates positions which have a single, fully conserved residue. Hyphens represent gaps inserted for optimal alignment. CYP82E4v2, *Nicotiana tabacum* nicotine demethylase (ABN42695.1); CYP82E3, *Nicotiana tomentosiformis* nicotine demethylase (ABM46919.1); CYP82C1p, *Glycine max* cytochrome P450 (AAB94590.1); CYP82G1, *Arabidopsis lyrata* DMNT/TMTT homoterpene synthase (XP_002885694.1). Accession numbers are shown in brackets.

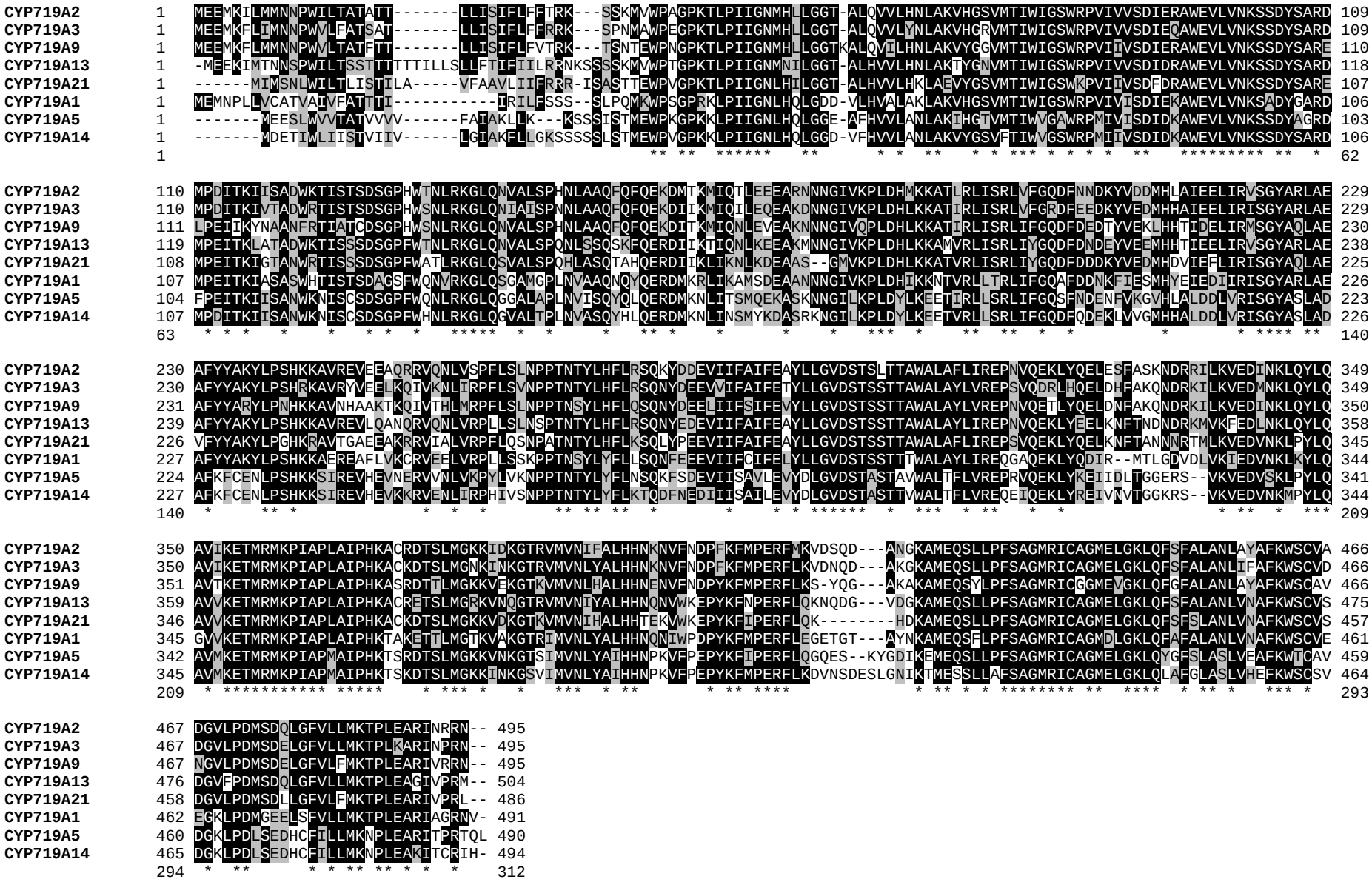


**Fig. S2b. Alignment of the deduced amino acid sequence of CYP719A21 with members of the CYP719A subfamily of cytochrome P450 oxygenases that have been functionally characterised as catalyzing methylenedioxy bridge-forming reactions.** Sequences were aligned in Clustal W (*43*). Residues identical in at least 50% of the sequences are shaded in black, similar residues in grey. An * (asterisk) underneath the

alignment indicates positions which have a single, fully conserved residue. Hyphens represent gaps inserted for optimal alignment. CYP719A2, *Eschscholzia californica* stylopine synthase (BAD98250 1); CYP719A3, *Eschscholzia californica* stylopine synthase (BAD98249.1); CYP719A5, *Eschscholzia californica* cheilanthifoline synthase (BAG75113.1); CYP719A9, *Eschscholzia californica* (BAG75114.1), CYP719A13, *Argemone mexicana* stylopine synthase (ABR14721.1); CYP719A14, *Argemone mexicana* cheilanthifoline synthase (ABR14722.1). Accession numbers are shown in brackets.

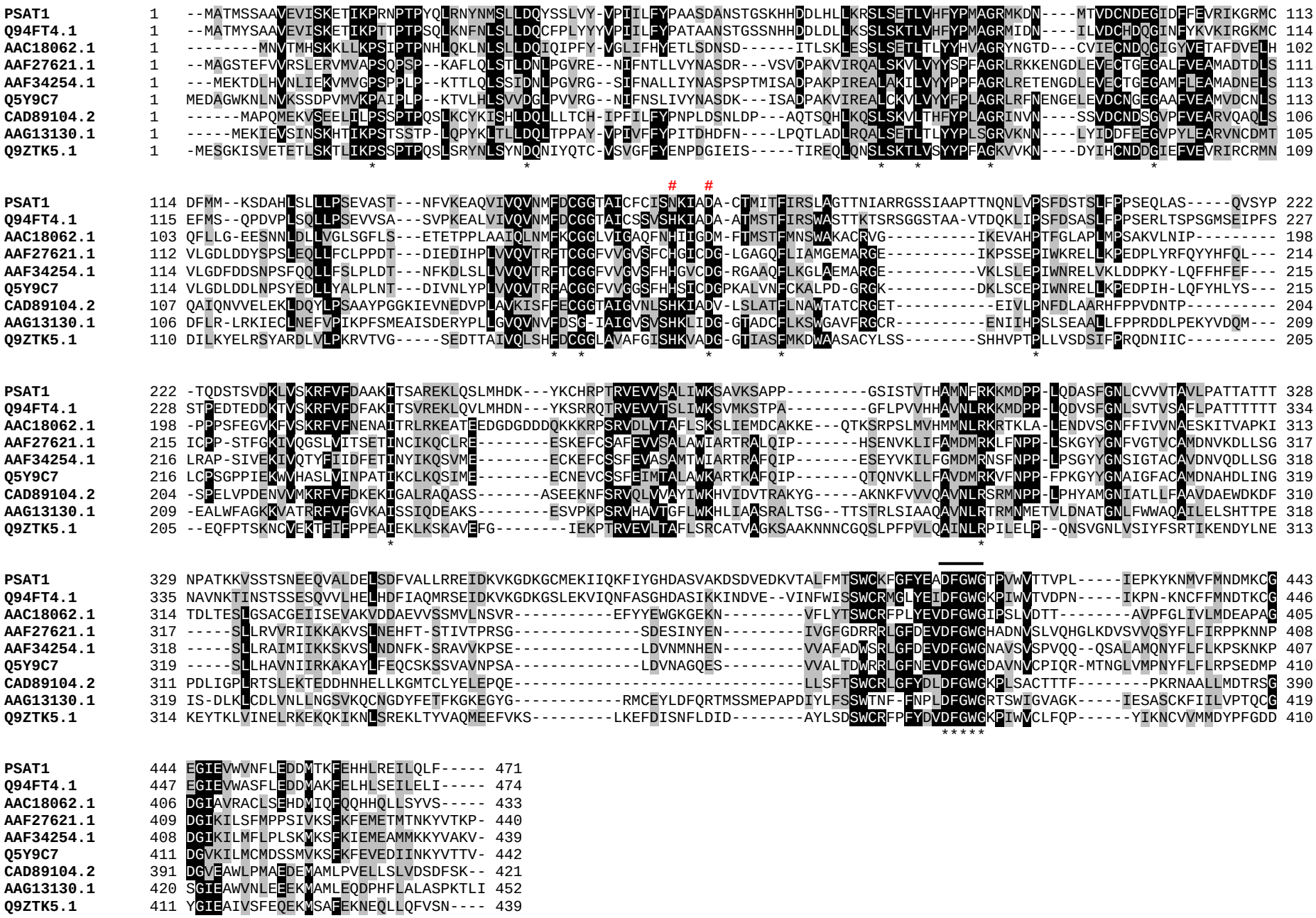


**Fig. S3. Sequence alignment of the deduced amino acid sequence of PSAT1 with functionally characterized acetyl and acyltransferases**

**from higher plants.** Sequences were aligned in Clustal W (*43*). Residues identical in at least 50% of the sequences are shaded in black, similar residues in grey. An * (asterisk) underneath the alignment indicates positions which have a single, fully conserved residue. Hyphens represent gaps inserted for optimal alignment. The position of the highly conserved histidine and aspartate of the HxxxD motif are indicated above the alignment by # (hash key). The highly conserved histidine is substituted by asparagine in the PSAT1 sequence. The black line above the alignment indicates the position of the highly conserved DFGWG motif which together with the HxxxD motif is a feature of BAHD-type acyltransferases. Q94FT4.1, *Papaver somniferum* salutaridinol 7-*O*-acetyltransferase; AAC18062.1, *Clarkia breweri* acetyl CoA: benzylalcohol acetyltransferase; AAF27621.1, Taxus cuspidata 10-deacetylbaccatin III-10-O-acetyl transferase; AAF34254.1, *Taxus cuspidate* taxadienol acetyl transferase; Q5Y9C7, *Taxus cuspidate* Taxoid-O-acetyltransferase; CAD89104.2, *Rauvolfia serpentine* vinorine synthase; AAG13130.1, *Fragaria x ananassa* vinorine synthase; Q9ZTK5.1, *Catharanthus roseus* Acetyl-coenzyme A:deacetylvindoline 4-O-acetyltransferase.

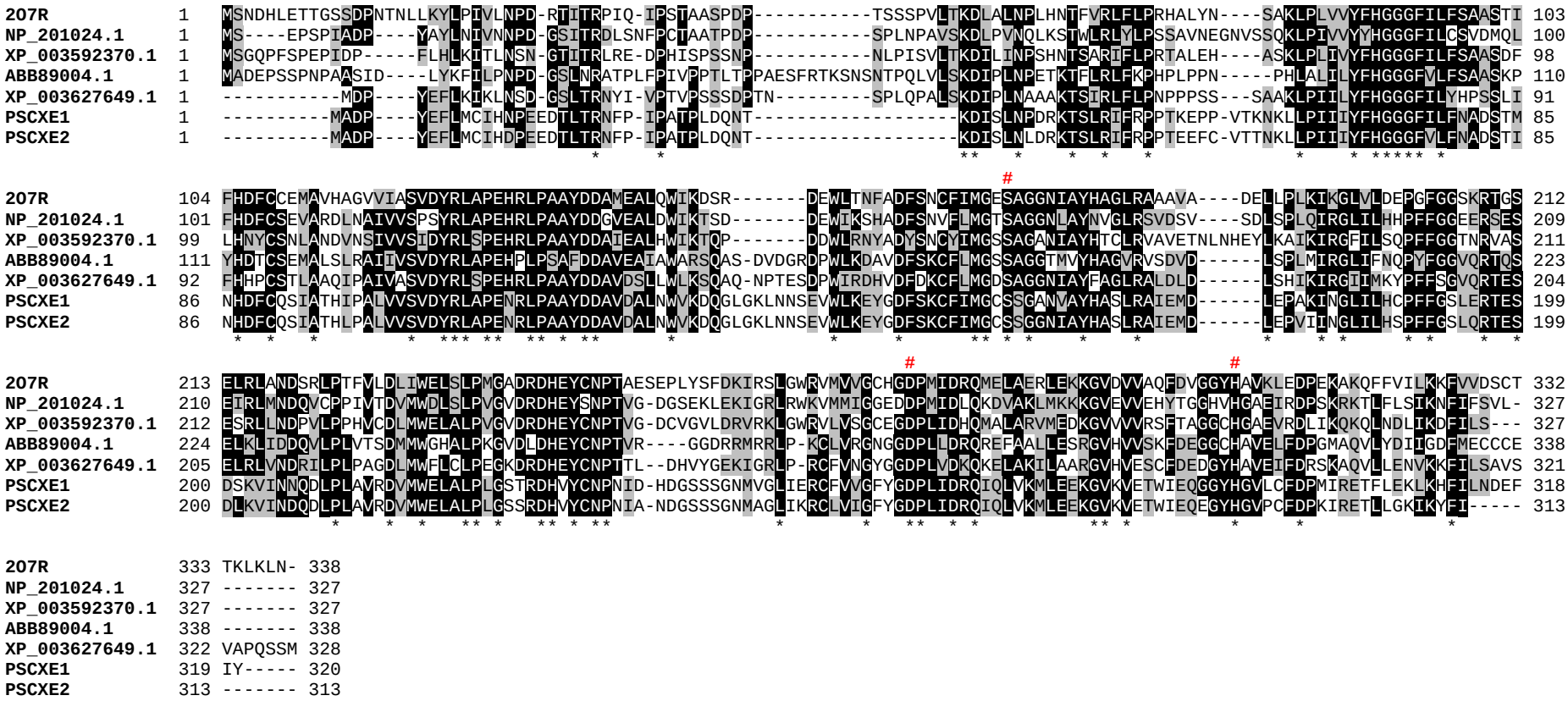


**Fig. S4. Sequence alignment of the deduced amino acid sequence of PSCXE1 and PSCXE2 with functionally characterized or annotated carboxylesterases and gibberellin receptor 1 proteins.** Sequences were aligned in Clustal W (*43*). Residues identical in at least 50% of the sequences are shaded in black, similar residues in grey. An * (asterisk) underneath the alignment indicates positions which have a single, fully conserved residue. Hyphens represent gaps inserted for optimal alignment. Catalytic residues are indicated above the alignment by # (hash key). PSCXE1 and PSCXE2 show homology to functionally characterized carboxylesterases and gibberellin receptor GID1. 2O7R **(**PDB**),** *Actinidia eriantha* chain A, plant carboxylesterase AeCXE1; NP_201024.1, *Arabidopsis thaliana* carboxyesterase 20; XP_003592370.1, *Medicago truncatula* CXE carboxylesterase; ABB89004.1, *Malus pumila* CXE carboxylesterase; XP_003627649.1, *Medicago truncatula* Gibberellin receptor GID1.

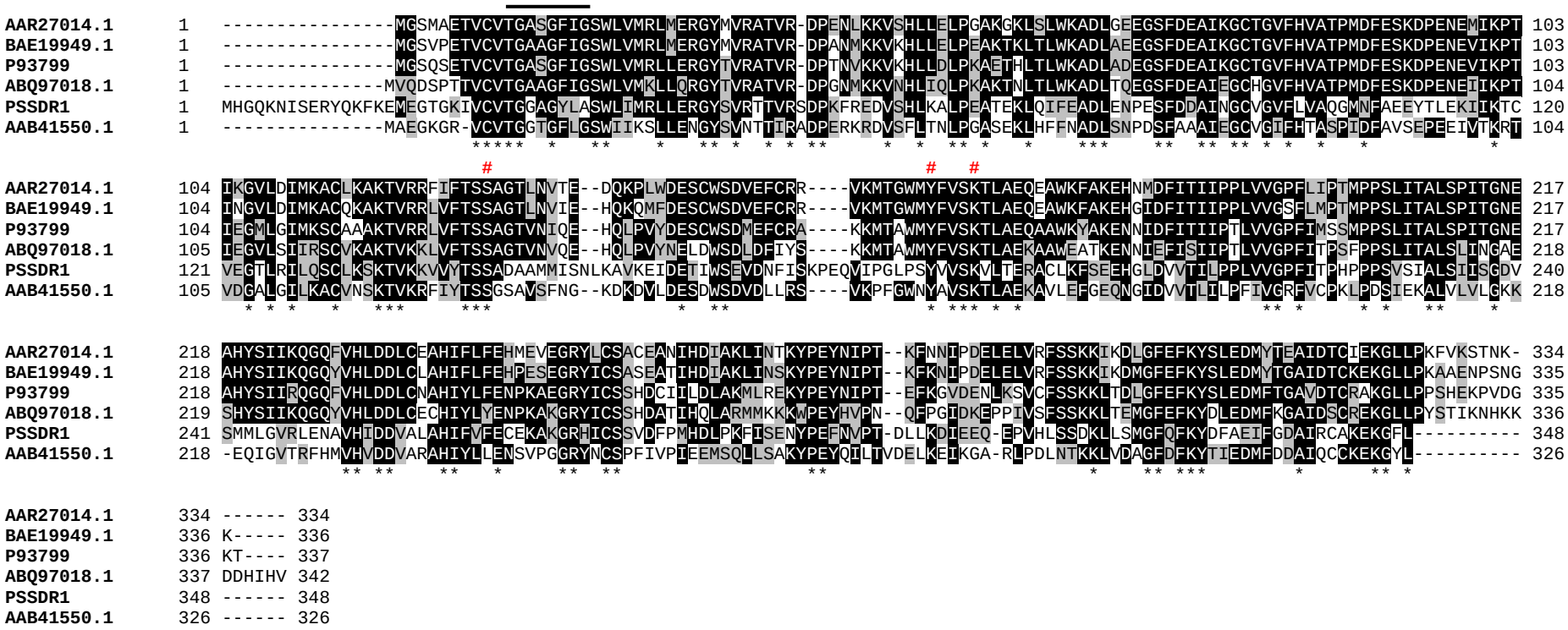


**Fig. S5. Sequence alignment of the deduced amino acid sequence of PSSDR1 with functionally characterized extended short chain dehydrogenase/reductases (eSDRs) from higher plants.** Sequences were aligned in Clustal W (*43*). Residues identical in at least 50% of the sequences are shaded in black, similar residues in grey. An * (asterisk) underneath the alignment indicates positions which have a single, fully conserved residue. Hyphens represent gaps inserted for optimal alignment. Catalytic residues are indicated above the alignment by # (hash key). PSSDR1 contains the YxxxK motif and an upstream serine which form the catalytic triad. The black line above the alignment indicates the position of the TGxxGxxG cofactor binding motif. AAR27014.1, *Medicago truncatula* dihydroflavanol-4-reductase; BAE19949.1, *Lotus japonicus* dihydroflavonol 4-reductase; P93799 (Swiss-Prot),*Vitis vinifera* Dihydroflavonol 4-reductase; ABQ97018.1, *Saussurea medusa* dihydroflavonol 4-reductase; AAB41550.1, *Medicago sativa* vestitone reductase.

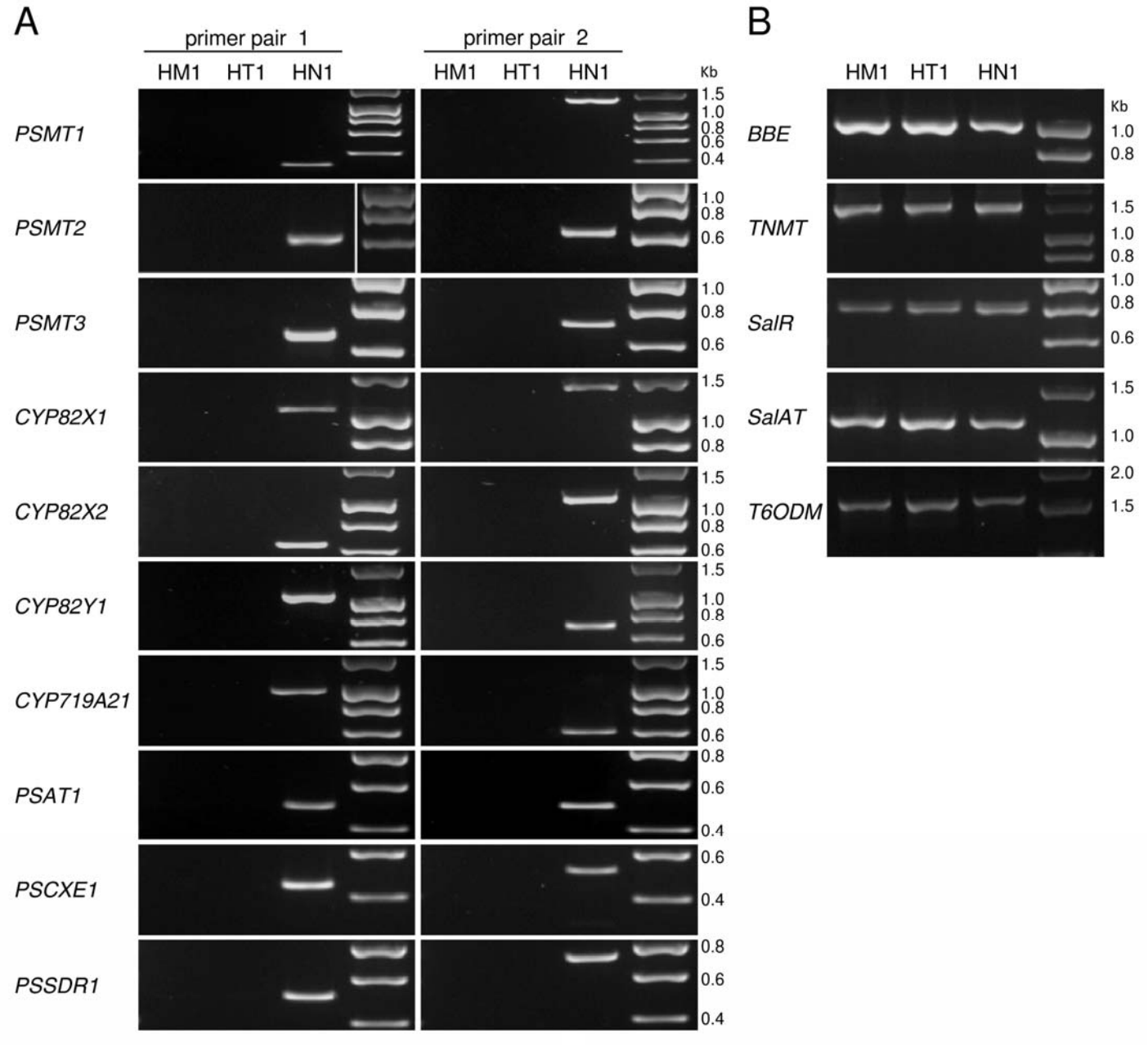


**Fig. S6. The ten genes exclusively expressed in the HN1 variety occur in the genome of HN1 but are absent from that of varieties HT1 and HM1.**

**(A)** Amplification of fragments from the ten genes exclusively expressed in HN1 using two different primer pairs. **(B)** Amplification of fragments of genes from the protoberberine and morphinan branch pathways that are expressed in all three varieties. Primers used are detailed in Table S8; HyperLadder I (Bioline Reagents, London, UK) was used as molecular size standard.

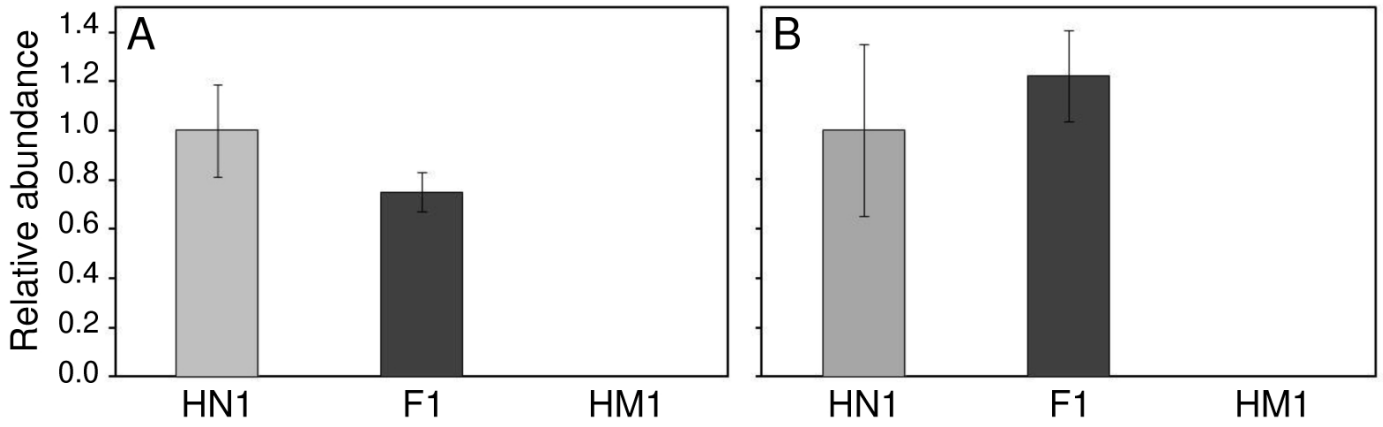


**Fig. S7. *PSMT1* and *PSMT2* mRNA abundance in upper stem sections of 8-9 week old HN1, HM1 and F1 (derived from HM1×HN1) plants determined by quantitative real-time PCR.** For each plant line at least three separate plants were sampled and three technical replicates were used per biological replicate. **(A)** Relative expression levels of *PSMT1* **(B)** Relative expression levels of *PSMT2*.

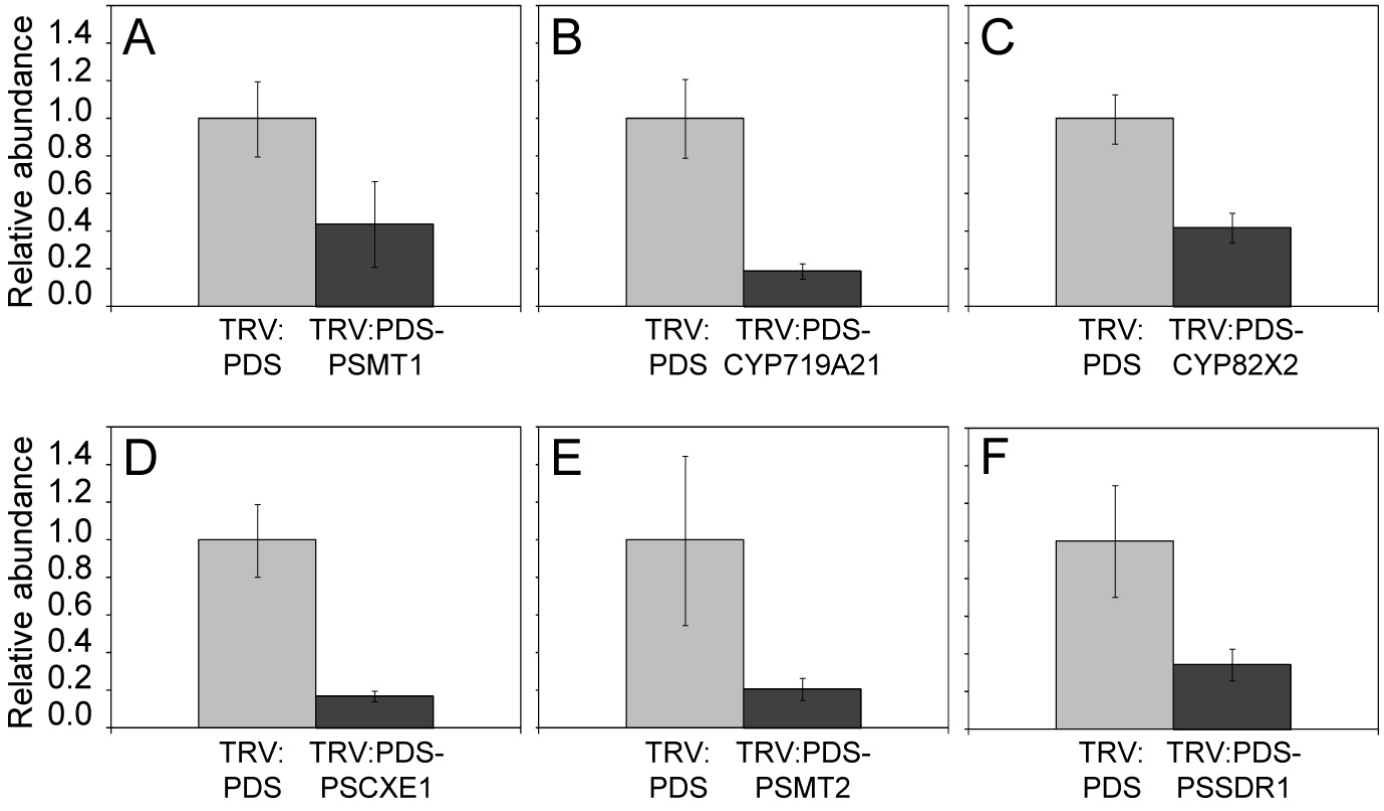


**Fig. S8. Target gene mRNA abundance in young leaves from 7 weeks old plants following VIGS as determined by quantitative real-time PCR.** mRNA levels are compared between plants inoculated with the TRV:PDS control vector and plants inoculated with constructs carrying the *PDS* gene fragment linked to the fragments of each of the target genes. For each construct at least three separate plants were sampled and three technical replicates were used per biological replicate. Note that for reasons of space pTRV2 has been abbreviated to TRV in the construct names.

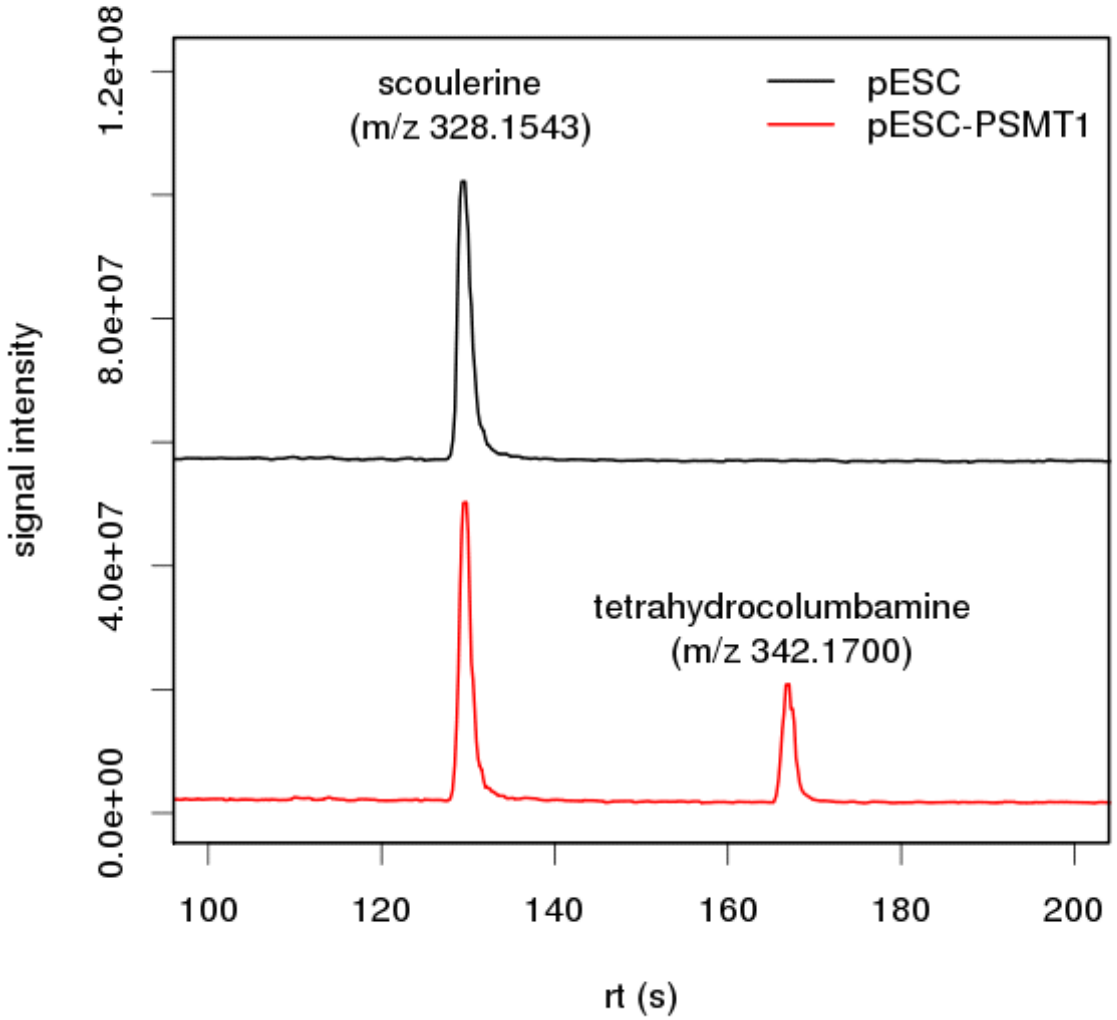


**Fig. S9. Heterologous expression of PSMT1 in yeast.** *PSMT1* was cloned into yeast vector pESC-TRP and transformed into ***Saccharomyces cerevisiae*** **G175**. Cultures were grown as previously described (*47*). Briefly, transformed cultures were grown on media containing glucose, washed and resuspended in 5mL induction medium in shake-flasks containing galactose with raffinose added as a carbon source. Six hours after induction, 15µM scoulerine was added to a subset of cultures. After 3 days, cultures were harvested by centrifugation and a 2µL aliquot of supernatant analysed by UPLC-MS. Off-set base peak chromatograms for the empty vector control and a representative assay are shown. Tetrahydrocolumbamine appeared in all four transformants and was not detectable in any controls (empty vector + substrate, wild-type ±substrate).

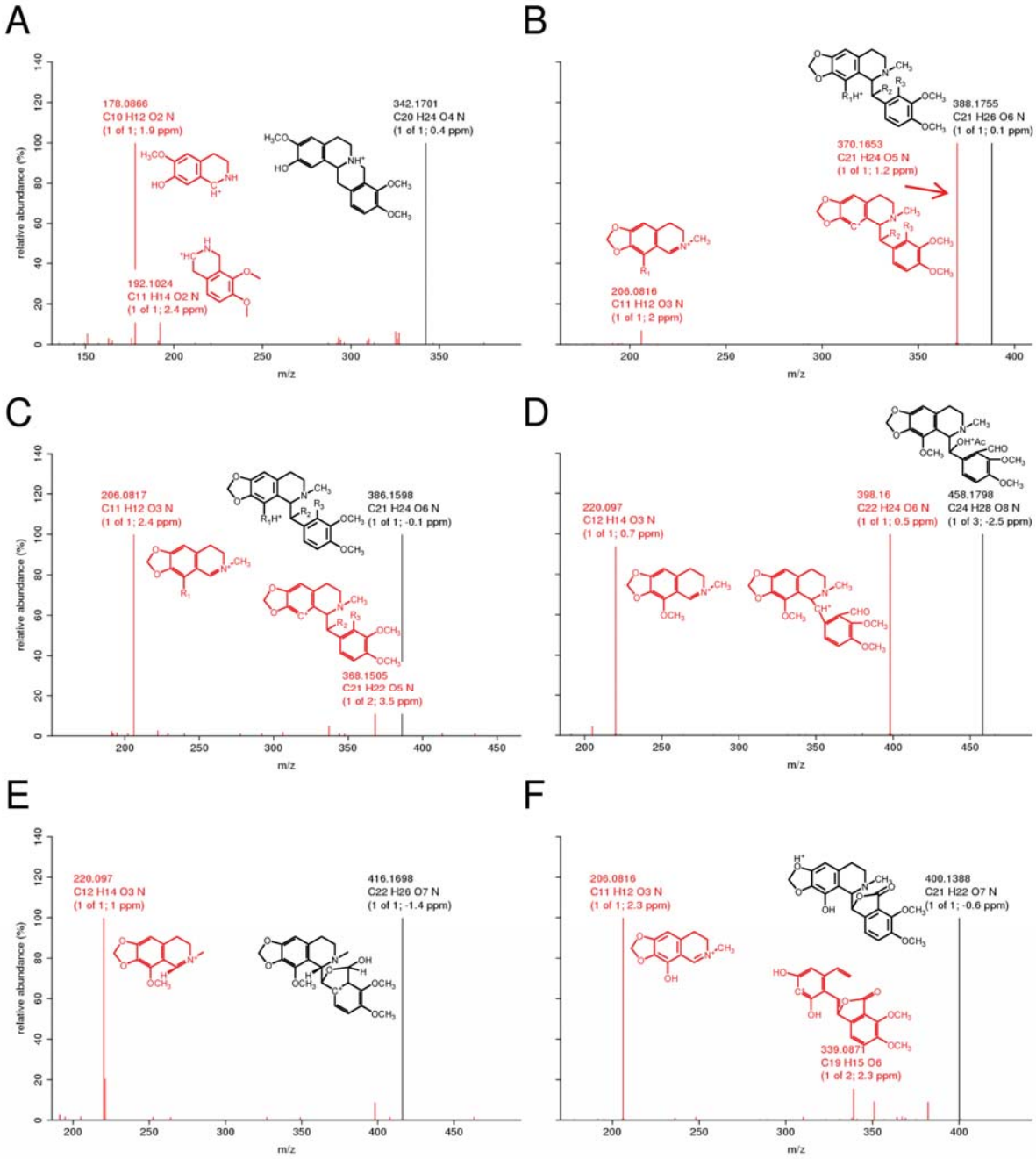


**Fig. S10. Evidence for putative identities of intermediates from VIGS experiments.** All panels show the mass spectra of the pseudomolecular parent ion at the chromatographic peak apex in black and corresponding MS2 fragmentation spectra in red, scaled to relative abundance. MS2 spectra were generated by targeting the parent ion with a isolation width of 3 m/z and using collisional isolation dissociation energy set to 35%. All mass spectra were obtained at a resolution setting of 7500. Text printed above selected diagnostic ions indicate the exact monoisotopic mass of the ion, the calculated formula within limits C=1:100, O=0:200, N=0:3 and H=1:200, and the number/total number of formulae returned within a 5ppm error window. Fragments were reconciled against theoretical fragments generated by submitting candidate parent structures to Mass Frontier software (version 5.01.2; HighChem, Bratislava, Slovakia). Candidate parent structures were derived from PubChem searches and the comprehensive review of *Papaver* spp. alkaloids (*48*). **(A)** Tetrahydrocolumbamine; this compound was characterized from a peak eluting at 174s from VIGS-silenced *CYP719A21*. Eight out of ten observed MS2 fragments were calculated as feasible by Mass Frontier; only the two most abundant diagnostic fragments are shown. **(B)** Secoberbine intermediate 1

(C21H25NO6); this compound was characterized from a peak eluting at 147s from VIGS-silenced *CYP82X2*. If $R_1$=OH, $R_2$=H, and $R_3$=$CH_2OH$, then this compound is narcotolinol which is consistent with both annotated fragments. Another candidate formula fit would be demethoxylated narcotindiol ($R_1$=H, $R_2$=OH, $R_3$=$CH_2OH$); however this structure would not form the observed fragment at 206.0816. **(C)** Secoberbine intermediate 2 (C21H23NO6); this compound was characterized from a peak eluting at 103s from VIGS-silenced *CYP82X2*. If $R_1$=OH , $R_2$=H, and $R_3$=CHO, then this compound would be a desmethylated derivative of macrantaldehyde. **(D)** Papaveroxine; this compound was characterized from a peak eluting at 214s from VIGS-silenced *PSCXE1*. The 398.1600 fragment observed is consistent with deacetylation. **(E)** Narcotinehemiacetal; this compound was characterized from a peak eluting at 121s from VIGS-silenced *PSSDR1*. **(F)** Narcotoline (4'-desmethylnoscapine); this compound was characterized from a peak eluting at 208s from VIGS-silenced *PSMT2*. Other isobaric possibilities were 6- or 7-desmethylnoscapine. However, the 206.0816 fragment observed is consistent with a hydroxylated 4' position. We were able to discount the alternative structures by comparing the candidate fragmentation spectra with that from synthetic 7-desmethylnoscapine, which eluted at a different retention time and lacked the characteristic 206.0816 fragment.

**Table S1. High noscapine variety (HN1) specific metabolites.**
Metabolites were extracted from ground capsule-straw of field-grown high noscapine (HN1; n=28), thebaine (HT1; n=38) and morphine (HM1; n=36) varieties. Extracts were analysed by UPLC-MS, and a global MassTag peak list generated by the Bioconductor package, XCMS (*37*). The global list was trimmed to remove background peaks, isotopes, adducts and fragments using custom R scripts and the CAMERA package *(39)*. The remaining peaks were annotated with calculated formulae and hits to known standards or putative compounds with matching candidate formulae. A total of 366 metabolites were reported as present ($p < 0.05$, ANOVA with Tukey's correction compared to a zero-value distribution), with 53 being HN1-specific. Above a threshold of 0.1% total profile, 10 metabolites were HN1-specific.

| MassTag[1] | Formula hits[2] (± 5ppm) | Formula[3] ([M+H]+) | Metabolite ID[4] | Capsule Yield[5] (% DW) | Capsule profile[6] (% total) | p value[7] | Fold change[8] |
|---|---|---|---|---|---|---|---|
| M414.1552T202 | 1 | C22H24NO7 | Noscapine | 1.7 ± 0.27 | 31 ± 3.2 | 1.40E-74 | 895 |
| M460.1969T187 | 1 | C24H30NO8 | Papaveroxinoline (putative) | 0.22 ± 0.077 | 3.9 ± 1.2 | 7.00E-43 | 3548 |
| M428.1707T98 | 1 | C23H26NO7 | | 0.078 ± 0.057 | 1.4 ± 0.97 | 8.90E-20 | 2889 |
| M400.1392T124 | 1 | C21H22NO7 | Narcotoline | 0.043 ± 0.01 | 0.77 ± 0.17 | 3.10E-58 | 1103 |
| M430.1493T99 | 1 | C22H24NO8 | | 0.018 ± 0.0026 | 0.31 ± 0.048 | 6.10E-78 | 13846 |
| M400.1395T170 | 1 | C21H22NO7 | NorNoscapine | 0.013 ± 0.0021 | 0.24 ± 0.044 | 7.60E-75 | 2653 |
| M446.1813T105 | 1 | C23H28NO8 | | 0.013 ± 0.0059 | 0.22 ± 0.1 | 4.70E-33 | 164557 |
| M342.1706T171 | 1 | C20H24NO4 | Tetrahydrocolumbamine | 0.0097 ± 0.0023 | 0.17 ± 0.041 | 7.90E-56 | 23 |
| M370.1650T158 | 1 | C21H24NO5 | Cryptopine or Demethoxymacrantaldehyde (both putative) | 0.0099 ± 0.013 | 0.17 ± 0.21 | 7.20E-09 | 2676 |
| M430.1500T86 | 1 | C22H24NO8 | | 0.0066 ± 0.00074 | 0.12 ± 0.016 | 8.40E-89 | 4714 |
| M222.1127T167 | 1 | C12H16NO3 | | 0.0051 ± 0.0021 | 0.091 ± 0.036 | 1.50E-37 | 2684 |
| M430.1764T109 | 1 | C25H24N3O4 | | 0.0051 ± 0.0022 | 0.091 ± 0.039 | 2.00E-35 | 113333 |
| M428.1349T162 | 2 | C22H22NO8 | | 0.0037 ± 0.00074 | 0.065 ± 0.018 | 2.20E-64 | 6379 |
| M386.1963T151 | 1 | C22H28NO5 | | 0.0034 ± 0.00091 | 0.06 ± 0.014 | 9.60E-54 | 24286 |
| M204.0659T205 | 1 | C11H10NO3 | | 0.003 ± 0.00047 | 0.052 ± 0.0069 | 8.90E-75 | 857 |
| M195.0655T85 | 1 | C10H11O4 | | 0.0027 ± 0.00086 | 0.048 ± 0.019 | 1.30E-45 | 129 |
| M211.0603T59 | 1 | C10H11O5 | | 0.0025 ± 0.0005 | 0.045 ± 0.011 | 9.80E-65 | 26882 |
| M343.1736T171 | 1 | C12H27N2O9 | | 0.002 ± 0.0005 | 0.035 ± 0.0089 | 6.60E-55 | 34 |
| M225.0760T205 | 1 | C11H13O5 | | 0.002 ± 0.00085 | 0.035 ± 0.013 | 2.90E-36 | 6250 |
| M459.1402T112 | 2 | C22H23N2O9 | | 0.0016 ± 0.00046 | 0.029 ± 0.0097 | 2.40E-50 | Inf |
| M445.1972T160 | 2 | C23H29N2O7 | | 0.0015 ± 0.00058 | 0.026 ± 0.0092 | 1.60E-39 | 45455 |
| M430.1500T149 | 1 | C22H24NO8 | | 0.0012 ± 0.00019 | 0.022 ± 0.0036 | 2.20E-74 | 21818 |

| | | | | | | | |
|---|---|---|---|---|---|---|---|
| M475.1350T84 | 2 | C22H23N2O10 | | 0.00098 ± 0.00035 | 0.018 ± 0.0075 | 2.50E-42 | Inf |
| M400.1394T149 | 1 | C21H22NO7 | 7-Desmethylnoscapine | 0.00089 ± 0.00024 | 0.016 ± 0.0047 | 2.00E-52 | Inf |
| M360.1292T64 | 1 | C15H22NO9 | | 0.00067 ± 0.00028 | 0.012 ± 0.0048 | 1.40E-36 | Inf |
| M458.1811T210 | 1 | C24H28NO8 | Papaveroxine (putative) | 0.00064 ± 0.0014 | 0.011 ± 0.024 | 1.00E-03 | 771 |
| M446.1809T166 | 1 | C23H28NO8 | | 0.00062 ± 0.00015 | 0.011 ± 0.0031 | 1.50E-57 | 12157 |
| M340.1545T229 | 1 | C20H22NO4 | Canadine | 0.00057 ± 0.00054 | 0.01 ± 0.01 | 2.10E-13 | 60 |
| M372.1809T120 | 1 | C21H26NO5 | Salutaridinol-7-O-acetate (putative) | 0.00058 ± 0.00017 | 0.01 ± 0.0026 | 3.30E-49 | Inf |
| M562.1925T122 | 2 | C27H32NO12 | | 0.00053 ± 0.00061 | 0.0092 ± 0.01 | 2.40E-10 | Inf |
| M206.0814T68 | 1 | C11H12NO3 | | 0.00049 ± 0.00013 | 0.0085 ± 0.0019 | 8.90E-52 | 327 |
| M520.2177T81 | 1 | C26H34NO10 | | 0.00047 ± 0.00039 | 0.0082 ± 0.0064 | 1.10E-16 | 9038 |
| M428.1342T77 | 2 | C22H22NO8 | | 0.00046 ± 0.000092 | 0.0083 ± 0.002 | 3.30E-65 | 5111 |
| M442.1495T157 | 2 | C23H24NO8 | | 0.00041 ± 0.00014 | 0.0072 ± 0.0023 | 1.50E-43 | 5857 |
| M444.1651T142 | 1 | C23H26NO8 | | 0.0004 ± 0.00022 | 0.0071 ± 0.0039 | 1.00E-27 | 5263 |
| M448.1866T106 | 1 | C25H26N3O5 | | 0.00032 ± 0.00025 | 0.0057 ± 0.0047 | 4.80E-18 | 3810 |
| M384.1443T159 | 1 | C21H22NO6 | | 0.0003 ± 0.000084 | 0.0054 ± 0.0014 | 6.40E-52 | Inf |
| M354.1704T118 | 1 | C21H24NO4 | N-methylcanadine (putative) | 0.00023 ± 0.00016 | 0.0041 ± 0.0026 | 6.00E-21 | 29 |
| M162.0549T29 | 1 | C9H8NO2 | | 0.00015 ± 0.00016 | 0.0028 ± 0.0031 | 2.40E-05 | 4 |
| M412.1390T78 | 2 | C22H22NO7 | | 0.00023 ± 0.000067 | 0.004 ± 0.0013 | 3.70E-49 | 6765 |
| M204.0656T140 | 1 | C11H10NO3 | | 0.00016 ± 0.000083 | 0.003 ± 0.0018 | 7.30E-29 | 70 |
| M476.1377T84 | 3 | C14H26N3O15 | | 0.00016 ± 0.000091 | 0.0029 ± 0.0018 | 1.90E-26 | Inf |
| M331.1286T72 | 1 | C17H19N2O5 | | 0.00011 ± 0.000087 | 0.002 ± 0.0018 | 5.90E-12 | 3 |
| M444.1654T199 | 1 | C23H26NO8 | | 0.00015 ± 0.000091 | 0.0026 ± 0.0016 | 2.40E-24 | Inf |
| M384.1444T222 | 1 | C21H22NO6 | | 0.00014 ± 0.000062 | 0.0026 ± 0.0012 | 9.70E-35 | 2121 |
| M236.1283T92 | 1 | C13H18NO3 | | 0.00012 ± 0.000073 | 0.0022 ± 0.0013 | 6.10E-25 | 1091 |
| M597.2962T164 | 2 | C36H41N2O6 | | 0.00011 ± 0.000079 | 0.0018 ± 0.0012 | 8.80E-18 | 10 |
| M204.0655T17 | 1 | C11H10NO3 | | 0.000052 ± 0.000051 | 0.00095 ± 0.00097 | 1.50E-03 | 2 |
| M396.1076T167 | 2 | C21H18NO7 | | 0.00007 ± 0.000052 | 0.0013 ± 0.0011 | 8.90E-19 | 119 |
| M192.1231T41 | 1 | C8H18NO4 | | 0.000054 ± 0.000033 | 0.00099 ± 0.00062 | 1.60E-21 | 15 |
| M384.1438T87 | 1 | C21H22NO6 | | 0.000062 ± 0.000077 | 0.0011 ± 0.0013 | 4.90E-09 | 73 |
| M706.2763T261 | 2 | C40H40N3O9 | | 0.000055 ± 0.000039 | 0.001 ± 0.00073 | 2.60E-20 | Inf |
| M238.1079T78 | 1 | C12H16NO4 | | 0.000041 ± 0.000061 | 0.00078 ± 0.0013 | 4.40E-07 | 293 |

Notes: MassTag[1] = mass-to-charge (m/z) value (M) followed by retention time (T) in seconds; Formula hits[2] = number of formula hits returned within limits of C = 1:100, H=1:200,O=0:20, N=0:3 and 5ppm error; Formula[3] = calculated formula of assumed pseudomolecular ion; Metabolite ID[4] = matches to standards or putative hits to literature

reported or hypothetical pathway compounds; Capsule yield[5] = where present morphine, codeine, oripavine, thebaine and noscapine are calculated using their respective standard curves and reported relative to dry weight. All other compounds were calculated using the thebaine standard curve. Values are means ± 1 standard deviation; Capsule profile[6] = individual metabolite yield / total metabolite yield x 100; p value[7] = ANOVA p-value result from HN1, HT1, HM1 comparisons where Tukeys's HSD correction was also < 0.05; Fold change[8] = minimum of HN1/HT1 or HN1/HM1 capsule yield value. All statistics and calculations were carried out using R 2.11.

**Table S2. Genotyping of F3 families derived from two F2 phenotypic classes: low noscapine and high noscapine.** The observed versus expected segregation ratios strongly support the hypothesis that individuals in the low noscapine F2 class are heterozygous for the HN1 gene cluster and individuals in the high noscapine class are homozygous.

| **Noscapine class and genotyping result of F2 individual** | **F3 seed family** (obtained through self-pollination of F2 individual) | **Number of F3 individuals genotyped** | **Observed segregation of gene cluster in F3 progeny** | | **Expected segregation in F3 if F2 low noscapine class is heterozygous and the high noscapine class is homozygous** | | **Chi-Square** | |
|---|---|---|---|---|---|---|---|---|
| | | | GC+ | GC- | GC+ | GC- | X-squared | p-value |
| **low** noscapine/GC+ | S-111809 | 28 | 18 | 10 | 21 | 7 | 1.714 | 0.190 |
| **low** noscapine/GC+ | S-111835 | 26 | 18 | 8 | 19.5 | 6.5 | 0.462 | 0.497 |
| **high** noscapine/GC+ | S-111714 | 28 | 28 | | 28 | | | |
| **high** noscapine/GC+ | S-111854 | 54 | 54 | | 54 | | | |

**Table S3. HN1-specific metabolites in the HN1 and HM1 x HN1 F1 generation.**
Metabolites were extracted from ground capsule straw as indicated in Fig. 2A. All metabolites that were absent in HM1 and significantly changed ($p < 0.05$, ANOVA with Tukey's HSD correction) in their % DW concentration between HN1 and the HM1 x HN1 F1 are tabulated. Table heading notes are as per Table S1. All HN1-specific metabolites except for salutaridinol-7-O-acetate were decreased in the F1realtive to HN1.

| MassTag[1] | Formula hits[2] (± 5ppm) | Formula[3] ([M+H]+) | Metabolite ID[4] | Capsule Yield[5] (% DW) | | p value[7] | Fold change[8] |
|---|---|---|---|---|---|---|---|
| | | | | HN1 | HM1 x HN1 F1 | | |
| M414.1539T195 | 1 | C22H24NO7 | Noscapine | 1.7 ± 0.38 | 0.2 ± 0.065 | 3.80E-23 | 0.12 |
| M460.1956T180 | 1 | C24H30NO8 | Papaveroxinoline (putative) | 0.38 ± 0.17 | 0.053 ± 0.021 | 1.10E-12 | 0.14 |
| M428.1698T88 | 1 | C23H26NO7 | | 0.16 ± 0.08 | 0.016 ± 0.0063 | 8.30E-12 | 0.10 |
| M400.1387T119 | 1 | C21H22NO7 | Narcotoline | 0.073 ± 0.024 | 0.0089 ± 0.0039 | 2.70E-17 | 0.12 |
| M430.1487T93 | 1 | C22H24NO8 | | 0.013 ± 0.0053 | 0.0012 ± 0.00048 | 3.90E-14 | 0.09 |
| M446.1804T101 | 1 | C23H28NO8 | | 0.013 ± 0.0072 | 0.00078 ± 0.00041 | 3.90E-10 | 0.06 |
| M400.1387T164 | 1 | C21H22NO7 | NorNoscapine | 0.0078 ± 0.0037 | 0.00071 ± 0.00023 | 2.80E-12 | 0.09 |
| M342.1697T165 | 1 | C20H24NO4 | Tetrahydrocolumbamine | 0.0048 ± 0.0024 | 0.0028 ± 0.0025 | 8.70E-07 | 0.58 |
| M222.1122T160 | 1 | C12H16NO3 | | 0.0032 ± 0.0015 | 0.00037 ± 0.00011 | 1.50E-12 | 0.12 |
| M386.1959T144 | 1 | C22H28NO5 | | 0.0022 ± 0.00096 | 0.0011 ± 0.00035 | 7.20E-12 | 0.50 |
| M430.1488T81 | 1 | C22H24NO8 | | 0.0029 ± 0.0013 | 0.00024 ± 0.000093 | 1.70E-13 | 0.08 |
| M445.1960T154 | 2 | C35H25 | | 0.0025 ± 0.0014 | 0.00024 ± 0.00011 | 1.50E-10 | 0.10 |
| M211.0600T57 | 1 | C10H11O5 | | 0.0024 ± 0.0014 | 0.000091 ± 0.000058 | 2.00E-10 | 0.04 |
| M340.1538T223 | 1 | C20H22NO4 | Canadine | 0.0017 ± 0.0012 | 0.00031 ± 0.0003 | 2.80E-07 | 0.18 |
| M430.1488T143 | 1 | C22H24NO8 | | 0.0016 ± 0.00062 | 0.00012 ± 0.000044 | 3.20E-15 | 0.08 |
| M372.1800T114 | 1 | C21H26NO5 | Salutaridinol-7-O-acetate (putative) | 0.00065 ± 0.00024 | 0.00087 ± 0.00028 | 1.80E-13 | 1.34 |
| M442.1488T151 | 1 | C23H24NO8 | | 0.0011 ± 0.00045 | 0.00016 ± 0.00016 | 2.10E-13 | 0.15 |
| M428.1346T155 | 2 | C22H22NO8 | | 0.001 ± 0.00052 | 0.000061 ± 0.000036 | 1.80E-11 | 0.06 |
| M400.1387T145 | 1 | C21H22NO7 | 6-Desmethylnoscapine (putative) | 0.001 ± 0.00029 | 0.00002 ± 0.00002 | 4.90E-20 | 0.02 |
| M220.0965T75 | 1 | C12H14NO3 | | 0.00084 ± 0.00038 | 0.0000029 ± 0.0000029 | 1.60E-13 | 0.00 |
| M562.1908T117 | 1 | C27H32NO12 | | 0.00077 ± 0.00093 | 0.0000027 ± 0.0000059 | 4.10E-04 | 0.00 |
| M384.1437T153 | 1 | C21H22NO6 | | 0.00058 ± 0.0002 | 0.000012 ± 0.000011 | 3.30E-17 | 0.02 |
| M414.1540T146 | 1 | C22H24NO7 | | 0.00046 ± 0.00018 | 0.000037 ± 0.000032 | 9.40E-15 | 0.08 |

| | | | | | | | |
|---|---|---|---|---|---|---|---|
| M460.1595T70 | 1 | C23H26NO9 | | 0.00041 ± 0.00011 | 0.000013 ± 0.000016 | 2.50E-20 | 0.03 |
| M428.1336T74 | 1 | C22H22NO8 | | 0.00036 ± 0.00022 | 0.0000011 ± 0.0000018 | 6.30E-10 | 0.00 |
| M400.1385T133 | 1 | C21H22NO7 | 7-Desmethylnoscapine | 0.00035 ± 0.00014 | 0.00000032 ± 0.0000011 | 1.10E-14 | 0.00 |
| M444.1647T192 | 1 | C23H26NO8 | | 0.00029 ± 0.00018 | 0.0000037 ± 0.0000041 | 1.40E-09 | 0.01 |
| M459.1390T106 | 2 | C34H19O2 | | 0.00021 ± 0.00022 | 0 ± 0 | 3.70E-05 | -Inf |
| M354.1696T104 | 1 | C21H24NO4 | N-methylcanadine (putative) | 0.000098 ± 0.000065 | 0 ± 0 | 5.90E-09 | -Inf |
| M354.1326T146 | 1 | C20H20NO5 | Protopine (putative) | 0.000092 ± 0.000057 | 0.0000013 ± 0.0000027 | 2.10E-09 | 0.01 |

**Table S4. Metabolites up-regulated in the HM1 x HN1 F1 generation relative to HM1.**
Metabolites were extracted from ground capsule straw as indicated in Fig. 2A. All metabolites that were significantly increased ($p < 0.05$, ANOVA with Tukey's HSD correction) in the HM1 x HN1 F1 % DW concentration relative to HM1 are tabulated. Table heading notes are as per Table S1.

| MassTag[1] | Formula hits[2] (± 5ppm) | Formula[3] ([M+H]+) | Metabolite ID[4] | Capsule Yield[5] (% DW) | | p value[7] | Fold change[8] |
|---|---|---|---|---|---|---|---|
| | | | | HM1 | HM1 x HN1 F1 | | |
| M286.1434T89 | 1 | C17H20NO3 | Morphine | 2.5 ± 0.76 | 3.4 ± 0.44 | 6.10E-08 | 1.36 |
| M330.1697T130 | 1 | C19H24NO4 | Reticuline | 0.01 ± 0.0029 | 0.015 ± 0.0033 | 1.10E-08 | 1.50 |
| M342.1697T165 | 1 | C20H24NO4 | Tetrahydrocolumbamine | 0.00011 ± 0.000061 | 0.0028 ± 0.0025 | 8.70E-07 | 25.45 |
| M370.1645T151 | 1 | C21H24NO5 | Cryptopine or Demethoxymacrantaldehyde (both putative) | 0 ± 0 | 0.002 ± 0.0019 | 2.00E-05 | Inf |
| M314.1747T170 | 1 | C19H24NO3 | | 0.00047 ± 0.0002 | 0.0014 ± 0.00026 | 1.70E-17 | 2.98 |
| M212.0916T265 | 1 | C10H14NO4 | | 0 ± 0 | 0.00069 ± 0.00017 | 2.60E-17 | Inf |
| M386.1959T144 | 1 | C22H28NO5 | | 0 ± 0 | 0.0011 ± 0.00035 | 7.20E-12 | Inf |
| M273.0858T75 | 1 | C14H13N2O4 | | 0.000086 ± 0.00017 | 0.0015 ± 0.00086 | 2.20E-09 | 17.44 |
| M220.1178T49 | 1 | C9H18NO5 | | 0.00021 ± 0.0002 | 0.0013 ± 0.00044 | 6.30E-10 | 6.19 |
| M198.1486T135 | 1 | C11H20NO2 | | 0.00033 ± 0.00015 | 0.0005 ± 0.00013 | 1.80E-05 | 1.52 |
| M372.1800T114 | 1 | C21H26NO5 | Salutaridinol-7-O-acetate (putative) | 0 ± 0 | 0.00087 ± 0.00028 | 1.80E-13 | Inf |
| M444.1644T137 | 1 | C23H26NO8 | | 0 ± 0 | 0.00058 ± 0.00042 | 2.10E-05 | Inf |
| M414.2329T85 | 1 | C17H36NO10 | | 0.00019 ± 0.00015 | 0.00061 ± 0.00021 | 1.20E-07 | 3.21 |
| M298.1071T66 | 1 | C17H16NO4 | | 0.00022 ± 0.000097 | 0.00047 ± 0.00016 | 6.80E-04 | 2.14 |
| M490.1906T53 | 2 | C34H24N3O | | 0.000046 ± 0.00011 | 0.00059 ± 0.00021 | 7.90E-10 | 12.83 |
| M312.1592T118 | 1 | C19H22NO3 | | 0.00025 ± 0.000094 | 0.00046 ± 0.000071 | 3.80E-10 | 1.84 |
| M406.2066T57 | 1 | C18H32NO9 | | 0.0002 ± 0.000085 | 0.00041 ± 0.000085 | 1.60E-06 | 2.05 |
| M388.1757T143 | 1 | C21H26NO6 | Narcotolinol (putative) | 0.000092 ± 0.000068 | 0.00028 ± 0.00007 | 1.90E-10 | 3.04 |
| M538.2847T72 | 2 | C37H36N3O | | 0.00014 ± 0.00011 | 0.00038 ± 0.00022 | 7.00E-04 | 2.71 |
| M448.2196T83 | 1 | C20H34NO10 | | 0.000043 ± 0.000073 | 0.00042 ± 0.00023 | 1.20E-05 | 9.77 |
| M438.2329T87 | 1 | C19H36NO10 | | 0.000016 ± 0.00005 | 0.00026 ± 0.00015 | 3.70E-07 | 16.25 |
| M362.2531T78 | 1 | C18H36NO6 | | 0.000064 ± 0.000061 | 0.00011 ± 0.000047 | 5.30E-04 | 1.72 |
| M269.1129T49 | 1 | C12H17N2O5 | | 0.000015 ± 0.000025 | 0.000069 ± 0.000043 | 6.20E-04 | 4.60 |
| M314.1020T57 | 1 | C17H16NO5 | | 0.0000047 ± 0.0000096 | 0.000037 ± 0.000023 | 3.80E-03 | 7.87 |

**Table S5. HN1 401Kb gene cluster region annotation** (provided as separate Excel file). **(A)** Positional information and type of ORFs predicted by the FGENESH gene prediction program (*42*) within the HN1 gene cluster genomic region. **(B)** Positional information and type of repetitive elements predicted by the RepeatMasker program (http://www.repeatmasker.org/cgi-bin/WEBRepeatMasker) within the HN1 gene cluster genomic region. **(C)** Summary repetitive elements predicted by RepeatMasker. All positional information refers to the HN1 gene cluster genomic region consensus sequence provided as a text file in Table S9.

**Table S6. Elements identified in the promoter region of the ten cluster genes** (provided as separate Excel file)**.** The 1Kb upstream region relative to the start of translation for each gene was compared against the PLACE database (*20*).

**Table S7. Significantly changed metabolite profile concentrations from VIGS experiments.**
Metabolites were extracted from ground capsule straw or leaf latex of n~10 VIGS *vs* control plants. All metabolites that were significantly changed ($p < 0.05$, ANOVA with Tukey's HSD correction) in their relative profile concentration are tabulated. The subset of metabolites shown in Fig. 4 were selected by applying objective statistical and threshold criteria (>0.05% total alkaloid profile, >2-fold positive change) to all samples and metabolites shown in this table. Table heading notes are as per Table S1.

| VIGs Construct | Tissue | MassTag[1] | Formula hits[2] (± 5ppm) | Formula[3] ([M+H]+) | Metabolite ID[4] | Profile[6] (% total) | | p value[7] | Fold change[8] |
|---|---|---|---|---|---|---|---|---|---|
| | | | | | | Control | VIGs Silenced | | |
| PSMT1 | Capsules | M346.2599T104 | 1 | C18H36NO5 | | 0.32 ± 0.13 | 0.15 ± 0.076 | 1.10E-02 | 0.47 |
| PSMT1 | Capsules | M328.1555T135 | 1 | C19H22NO4 | Scoulerine | 0.0042 ± 0.0033 | 0.064 ± 0.056 | 1.00E-06 | 15.24 |
| PSMT1 | Capsules | M611.2773T194 | 3 | C23H47O18 | | 0.0015 ± 0.0012 | 0.024 ± 0.019 | 7.30E-08 | 16.00 |
| PSMT1 | Capsules | M329.1590T135 | 1 | C16H25O7 | | 0.00015 ± 0.00034 | 0.01 ± 0.011 | 8.50E-06 | 66.67 |
| PSMT1 | Capsules | M502.2085T87 | 1 | C26H32NO9 | | 0.000091 ± 0.000067 | 0.008 ± 0.0069 | 2.50E-08 | 87.91 |
| PSMT1 | Capsules | M340.1558T87 | 1 | C20H22NO4 | Papaverine (putative) | 0.000014 ± 0.000024 | 0.0054 ± 0.0052 | 7.60E-07 | 385.71 |
| PSMT1 | Capsules | M342.1346T120 | 1 | C19H20NO5 | | 0.00049 ± 0.00022 | 0.002 ± 0.0015 | 1.60E-07 | 4.08 |
| PSMT1 | Capsules | M327.1350T81 | 1 | C18H19N2O4 | | 0 ± 0 | 0.0009 ± 0.00099 | 1.90E-05 | Inf |
| PSMT1 | Latex | M302.1609T88 | 1 | C14H24NO6 | | 0.81 ± 0.37 | 0.9 ± 0.39 | 1.00E-20 | 1.11 |
| PSMT1 | Latex | M328.1555T134 | 1 | C19H22NO4 | Scoulerine | 0.00004 ± 0.00013 | 0.61 ± 0.92 | 8.60E-06 | 15250.00 |
| PSMT1 | Latex | M330.1713T138 | 1 | C19H24NO4 | Reticuline | 0.022 ± 0.018 | 0.11 ± 0.049 | 5.00E-03 | 5.00 |
| PSMT1 | Latex | M223.0973T84 | 1 | C12H15O4 | | 0.073 ± 0.03 | 0.081 ± 0.035 | 4.50E-11 | 1.11 |
| PSMT1 | Latex | M611.2774T196 | 3 | C23H47O18 | | 0.00012 ± 0.00039 | 0.05 ± 0.068 | 1.30E-06 | 416.67 |
| PSMT1 | Latex | M314.1763T181 | 1 | C19H24NO3 | | 0.0018 ± 0.0024 | 0.032 ± 0.022 | 7.70E-03 | 17.78 |
| CYP719A21 | Capsules | M342.1712T175 | 1 | C20H24NO4 | Tetrahydrocolumbamine | 0.046 ± 0.02 | 0.19 ± 0.17 | 1.10E-02 | 4.13 |

| | | | | | | | | | |
|---|---|---|---|---|---|---|---|---|---|
| CYP719A21 | Capsules | M256.0605T79 | 1 | C14H10NO4 | | 0.0012 ± 0.0013 | 0.042 ± 0.032 | 3.40E-06 | 35.00 |
| CYP719A21 | Capsules | M343.1745T175 | 1 | C17H27O7 | | 0.0093 ± 0.0042 | 0.041 ± 0.036 | 1.10E-02 | 4.41 |
| CYP719A21 | Capsules | M518.2399T75 | 1 | C27H36NO9 | | 0.000005 ± 0.000013 | 0.0089 ± 0.019 | 1.50E-02 | 1780.00 |
| CYP719A21 | Capsules | M272.0554T75 | 1 | C14H10NO5 | | 0.00014 ± 0.00018 | 0.0048 ± 0.0039 | 1.90E-04 | 34.29 |
| CYP719A21 | Capsules | M344.1772T175 | 1 | C22H22N3O | | 0.00047 ± 0.00049 | 0.0044 ± 0.0048 | 9.10E-03 | 9.36 |
| CYP719A21 | Capsules | M504.2240T127 | 1 | C26H34NO9 | | 0.0000095 ± 0.000016 | 0.0042 ± 0.0086 | 7.60E-03 | 442.11 |
| CYP719A21 | Capsules | M625.2934T218 | 3 | C24H49O18 | | 0.00011 ± 0.00012 | 0.0027 ± 0.0026 | 7.50E-05 | 24.55 |
| CYP719A21 | Capsules | M404.2078T174 | 1 | C22H30NO6 | | 0.0016 ± 0.00035 | 0.0024 ± 0.0012 | 2.50E-14 | 1.50 |
| CYP719A21 | Capsules | M372.1876T62 | 1 | C14H30NO10 | | 0.00023 ± 0.00025 | 0.0016 ± 0.0018 | 4.80E-02 | 6.96 |
| CYP719A21 | Capsules | M538.2453T157 | 2 | C18H40N3O15 | | 0 ± 0 | 0.0013 ± 0.0011 | 3.30E-05 | Inf |
| CYP719A21 | Capsules | M681.3207T253 | 4 | C45H45O6 | | 0 ± 0 | 0.00072 ± 0.00073 | 5.60E-04 | Inf |
| CYP719A21 | Latex | M234.1346T86 | 1 | C10H20NO5 | | 0.64 ± 0.27 | 0.77 ± 0.33 | 3.70E-19 | 1.20 |
| CYP719A21 | Latex | M342.1712T175 | 1 | C20H24NO4 | Tetrahydrocolumbamine | 0.008 ± 0.012 | 0.28 ± 0.33 | 5.80E-03 | 35.00 |
| CYP719A21 | Latex | M223.0973T84 | 1 | C12H15O4 | | 0.073 ± 0.03 | 0.088 ± 0.034 | 4.50E-11 | 1.21 |
| CYP719A21 | Latex | M280.1773T65 | 1 | C12H26NO6 | | 0.074 ± 0.032 | 0.083 ± 0.041 | 5.40E-06 | 1.12 |
| CYP719A21 | Latex | M288.1453T73 | 1 | C13H22NO6 | | 0.05 ± 0.021 | 0.055 ± 0.019 | 4.10E-12 | 1.10 |
| CYP82X2 | Capsules | M388.1771T152 | 1 | C21H26NO6 | Narcotolinol (putative) | 0.005 ± 0.002 | 0.4 ± 0.23 | 8.50E-07 | 80.00 |
| CYP82X2 | Capsules | M462.2134T102 | 1 | C24H32NO8 | | 0.071 ± 0.035 | 0.21 ± 0.084 | 3.10E-03 | 2.96 |
| CYP82X2 | Capsules | M386.1610T105 | 1 | C21H24NO6 | Demethoxyhydroxy-macrantaldehyde (putative) | 0.00079 ± 0.00064 | 0.21 ± 0.11 | 2.70E-08 | 265.82 |
| CYP82X2 | Capsules | M370.1663T88 | 1 | C21H24NO5 | Cryptopine or Demethoxymacrantaldehyde (both putative) | 0.0034 ± 0.0015 | 0.19 ± 0.1 | 1.50E-17 | 55.88 |
| CYP82X2 | Capsules | M314.1763T180 | 1 | C19H24NO3 | | 0.03 ± 0.0051 | 0.099 ± 0.042 | 5.20E-04 | 3.30 |
| CYP82X2 | Capsules | M400.1764T221 | 1 | C22H26NO6 | N-Methopapavaberbine (putative) | 0 ± 0 | 0.012 ± 0.0077 | 8.70E-07 | Inf |
| CYP82X2 | Capsules | M318.1353T68 | 1 | C17H20NO5 | | 0.0024 ± 0.0012 | 0.0099 ± 0.0058 | 5.50E-03 | 4.13 |
| CYP82X2 | Capsules | M595.2821T267 | 3 | C23H47O17 | | 0.0000077 ± 0.00002 | 0.0083 ± 0.011 | 6.40E-03 | 1077.92 |
| CYP82X2 | Capsules | M372.1722T88 | 1 | C23H22N3O2 | | 0.0000056 ± 0.000015 | 0.0052 ± 0.0027 | 2.70E-17 | 928.57 |
| CYP82X2 | Capsules | M581.2662T232 | 2 | C22H45O17 | | 0.000036 ± 0.000052 | 0.005 ± 0.0077 | 1.30E-02 | 138.89 |
| CYP82X2 | Capsules | M671.2995T192 | 4 | C43H43O7 | | 0.00001 ± 0.000027 | 0.0047 ± 0.0053 | 6.80E-04 | 470.00 |
| CYP82X2 | Capsules | M476.2291T137 | 1 | C25H34NO8 | | 0.00092 ± 0.00067 | 0.0041 ± 0.0029 | 1.10E-02 | 4.46 |
| CYP82X2 | Capsules | M628.3123T205 | 2 | C34H46NO10 | | 0.000051 ± 0.00006 | 0.0039 ± 0.0064 | 2.50E-02 | 76.47 |
| CYP82X2 | Capsules | M331.1299T73 | 1 | C17H19N2O5 | | 0.00035 ± 0.00045 | 0.0033 ± 0.0034 | 3.10E-02 | 9.43 |
| CYP82X2 | Capsules | M179.0712T84 | 1 | C10H11O3 | | 0.00014 ± 0.00025 | 0.0032 ± 0.0019 | 2.30E-07 | 22.86 |

| | | | | | | | | | |
|---|---|---|---|---|---|---|---|---|---|
| CYP82X2 | Capsules | M301.1275T90 | 1 | C14H21O7 | | 0.00057 ± 0.00084 | 0.003 ± 0.0019 | 1.70E-03 | 5.26 |
| CYP82X2 | Capsules | M402.1553T70 | 1 | C21H24NO7 | | 0.000086 ± 0.000079 | 0.003 ± 0.0028 | 2.20E-12 | 34.88 |
| CYP82X2 | Capsules | M550.2298T125 | 2 | C27H36NO11 | | 0 ± 0 | 0.003 ± 0.0046 | 4.80E-04 | Inf |
| CYP82X2 | Capsules | M677.2883T184 | 3 | C27H49O19 | | 0 ± 0 | 0.0024 ± 0.003 | 1.90E-03 | Inf |
| CYP82X2 | Capsules | M151.0758T89 | 1 | C9H11O2 | | 0.000013 ± 0.000022 | 0.0023 ± 0.0014 | 6.80E-08 | 176.92 |
| CYP82X2 | Capsules | M597.2984T165 | 3 | C23H49O17 | | 0.00056 ± 0.00044 | 0.0022 ± 0.0021 | 4.40E-03 | 3.93 |
| CYP82X2 | Capsules | M392.1712T91 | 1 | C20H26NO7 | | 0.000031 ± 0.000046 | 0.0019 ± 0.0015 | 9.20E-04 | 61.29 |
| CYP82X2 | Capsules | M372.1453T110 | 1 | C20H22NO6 | | 0 ± 0 | 0.0016 ± 0.00092 | 1.00E-07 | Inf |
| CYP82X2 | Capsules | M402.1924T236 | 1 | C22H28NO6 | Macrantaline (putative) | 0 ± 0 | 0.0014 ± 0.0014 | 1.40E-04 | Inf |
| CYP82X2 | Capsules | M216.1242T77 | 1 | C10H18NO4 | | 0 ± 0 | 0.0014 ± 0.00092 | 1.30E-07 | Inf |
| CYP82X2 | Capsules | M669.2828T172 | 3 | C25H49O20 | | 0 ± 0 | 0.00083 ± 0.00093 | 4.70E-04 | Inf |
| CYP82X2 | Capsules | M384.1455T162 | 1 | C21H22NO6 | | 0.0087 ± 0.0011 | 0.00038 ± 0.00054 | 2.20E-04 | 0.04 |
| CYP82X2 | Latex | M302.1609T88 | 1 | C14H24NO6 | | 0.81 ± 0.37 | 0.81 ± 0.18 | 1.00E-20 | 1.00 |
| CYP82X2 | Latex | M234.1346T86 | 1 | C10H20NO5 | | 0.64 ± 0.27 | 0.67 ± 0.17 | 3.70E-19 | 1.05 |
| CYP82X2 | Latex | M388.1770T148 | 1 | C21H26NO6 | Narcotolinol (putative) | 0.000071 ± 0.00015 | 0.34 ± 0.19 | 3.80E-12 | 4788.73 |
| CYP82X2 | Latex | M386.1610T104 | 1 | C21H24NO6 | Demethoxyhydroxy-macrantaldehyde (putative) | 0.00003 ± 0.000096 | 0.26 ± 0.13 | 4.40E-14 | 8666.67 |
| CYP82X2 | Latex | M228.1966T182 | 1 | C13H26NO2 | | 0.089 ± 0.041 | 0.09 ± 0.027 | 2.20E-02 | 1.01 |
| CYP82X2 | Latex | M313.1444T263 | 1 | C19H21O4 | | 0.11 ± 0.053 | 0.078 ± 0.017 | 8.20E-05 | 0.71 |
| CYP82X2 | Latex | M223.0973T84 | 1 | C12H15O4 | | 0.073 ± 0.03 | 0.074 ± 0.017 | 4.50E-11 | 1.01 |
| CYP82X2 | Latex | M280.1773T65 | 1 | C12H26NO6 | | 0.074 ± 0.032 | 0.066 ± 0.016 | 5.40E-06 | 0.89 |
| CYP82X2 | Latex | M330.1712T263 | 1 | C19H24NO4 | Salutaridinol (putative) | 0.081 ± 0.033 | 0.055 ± 0.017 | 1.50E-02 | 0.68 |
| CYP82X2 | Latex | M288.1453T73 | 1 | C13H22NO6 | | 0.05 ± 0.021 | 0.053 ± 0.012 | 4.10E-12 | 1.06 |
| CYP82X2 | Latex | M190.1444T66 | 1 | C9H20NO3 | | 0.022 ± 0.0089 | 0.025 ± 0.0058 | 6.60E-09 | 1.14 |
| CYP82X2 | Latex | M294.2076T131 | 1 | C17H28NO3 | | 0.014 ± 0.0057 | 0.017 ± 0.0043 | 5.20E-05 | 1.21 |
| CYP82X2 | Latex | M334.2234T73 | 1 | C16H32NO6 | | 0.015 ± 0.0062 | 0.0088 ± 0.0021 | 1.50E-04 | 0.59 |
| PSCXE1 | Capsules | M458.1794T212 | 2 | C19H28N3O10 | Papaveroxine (putative) | 0.071 ± 0.039 | 14 ± 8.3 | 6.70E-18 | 197.18 |
| PSCXE1 | Capsules | M569.2635T132 | 2 | C34H37N2O6 | Pseudomorphine | 0.14 ± 0.033 | 0.31 ± 0.14 | 1.10E-03 | 2.21 |
| PSCXE1 | Capsules | M444.1641T143 | 1 | C23H26NO8 | | 0.058 ± 0.032 | 0.31 ± 0.17 | 1.90E-10 | 5.34 |
| PSCXE1 | Capsules | M569.2636T170 | 2 | C34H37N2O6 | | 0.032 ± 0.0084 | 0.064 ± 0.025 | 1.70E-02 | 2.00 |
| PSCXE1 | Capsules | M460.1956T209 | 1 | C24H30NO8 | Papaveroxinoline (putative) | 0.0023 ± 0.0011 | 0.04 ± 0.025 | 8.30E-13 | 17.39 |
| PSCXE1 | Capsules | M749.3061T255 | 1 | C43H45N2O10 | | 0.00015 ± 0.00019 | 0.034 ± 0.031 | 4.40E-10 | 226.67 |
| PSCXE1 | Capsules | M458.1964T225 | 2 | C28H28NO5 | | 0.000022 ± 0.000046 | 0.028 ± 0.03 | 4.30E-07 | 1272.73 |
| PSCXE1 | Capsules | M474.1743T172 | 2 | C19H28N3O11 | | 0.0057 ± 0.0033 | 0.012 ± 0.0072 | 7.30E-06 | 2.11 |

| | | | | | | | | | |
|---|---|---|---|---|---|---|---|---|---|
| PSCXE1 | Capsules | M683.2957T257 | 2 | C39H43N2O9 | | 0.0000068 ± 0.00002 | 0.012 ± 0.0076 | 2.20E-16 | 1764.71 |
| PSCXE1 | Capsules | M478.1903T64 | 3 | C33H24N3O | | 0.0083 ± 0.0024 | 0.011 ± 0.0038 | 4.50E-03 | 1.33 |
| PSCXE1 | Capsules | M707.2954T265 | 2 | C41H43N2O9 | | 0.0000069 ± 0.000021 | 0.01 ± 0.0094 | 6.40E-10 | 1449.28 |
| PSCXE1 | Capsules | M429.1722T202 | 2 | C15H29N2O12 | | 0.0022 ± 0.0011 | 0.009 ± 0.0078 | 4.80E-07 | 4.09 |
| PSCXE1 | Capsules | M400.1382T151 | 1 | C21H22NO7 | 7-Desmethylnoscapine | 0.022 ± 0.0048 | 0.0083 ± 0.0054 | 2.50E-02 | 0.38 |
| PSCXE1 | Capsules | M284.1275T64 | 1 | C17H18NO3 | Morphinone (putative) | 0.0042 ± 0.0015 | 0.007 ± 0.0042 | 1.80E-03 | 1.67 |
| PSCXE1 | Capsules | M767.3171T242 | 1 | C43H47N2O11 | | 0 ± 0 | 0.007 ± 0.0074 | 4.60E-07 | Inf |
| PSCXE1 | Capsules | M583.2431T121 | 2 | C34H35N2O7 | | 0.0015 ± 0.00074 | 0.0061 ± 0.0072 | 1.20E-02 | 4.07 |
| PSCXE1 | Capsules | M749.3062T250 | 1 | C43H45N2O10 | | 0 ± 0 | 0.0058 ± 0.0063 | 3.30E-07 | Inf |
| PSCXE1 | Capsules | M444.1636T89 | 1 | C18H26N3O10 | | 0.000012 ± 0.000035 | 0.0053 ± 0.0029 | 9.00E-19 | 441.67 |
| PSCXE1 | Capsules | M683.2954T240 | 2 | C39H43N2O9 | | 0 ± 0 | 0.0053 ± 0.0032 | 9.60E-17 | Inf |
| PSCXE1 | Capsules | M474.1743T158 | 2 | C19H28N3O11 | | 0.0000077 ± 0.000023 | 0.0053 ± 0.0057 | 8.60E-09 | 688.31 |
| PSCXE1 | Capsules | M397.1747T181 | 1 | C22H25N2O5 | | 0 ± 0 | 0.0043 ± 0.003 | 1.90E-15 | Inf |
| PSCXE1 | Capsules | M723.2911T251 | 1 | C41H43N2O10 | | 0 ± 0 | 0.0036 ± 0.003 | 1.40E-10 | Inf |
| PSCXE1 | Capsules | M463.2219T112 | 1 | C27H31N2O5 | | 0 ± 0 | 0.0028 ± 0.0033 | 3.40E-05 | Inf |
| PSCXE1 | Capsules | M384.1435T160 | 1 | C21H22NO6 | | 0.011 ± 0.002 | 0.00062 ± 0.00078 | 1.50E-05 | 0.06 |
| PSCXE1 | Latex | M458.1792T221 | 1 | C19H28N3O10 | Papaveroxine (putative) | 0.14 ± 0.13 | 14 ± 6.8 | 1.20E-12 | 100.00 |
| PSCXE1 | Latex | M444.1635T150 | 1 | C18H26N3O10 | | 0.0024 ± 0.0028 | 0.087 ± 0.055 | 8.70E-07 | 36.25 |
| PSCXE1 | Latex | M428.1694T211 | 1 | C23H26NO7 | | 0.0016 ± 0.0021 | 0.011 ± 0.0081 | 7.70E-06 | 6.88 |
| PSSDR1 | Capsules | M416.1684T206 | 1 | C17H26N3O9 | Narcotinehemiacetal (putative) | 0.0003 ± 0.00035 | 2.2 ± 1.9 | 1.10E-08 | 7333.33 |
| PSSDR1 | Capsules | M222.1120T169 | 1 | C12H16NO3 | | 0.051 ± 0.012 | 0.14 ± 0.083 | 1.10E-07 | 2.75 |
| PSSDR1 | Capsules | M378.1752T71 | 1 | C16H28NO9 | | 0.00021 ± 0.00012 | 0.081 ± 0.06 | 1.50E-12 | 385.71 |
| PSSDR1 | Capsules | M220.0964T76 | 1 | C12H14NO3 | | 0.015 ± 0.0032 | 0.065 ± 0.034 | 2.70E-11 | 4.33 |
| PSSDR1 | Capsules | M506.2159T183 | 2 | C29H32NO7 | | 0.000093 ± 0.00011 | 0.054 ± 0.03 | 1.60E-16 | 580.65 |
| PSSDR1 | Capsules | M506.2159T193 | 2 | C29H32NO7 | | 0.000032 ± 0.00005 | 0.035 ± 0.02 | 1.90E-17 | 1093.75 |
| PSSDR1 | Capsules | M803.3527T252 | 2 | C47H51N2O10 | | 0.0000074 ± 0.000022 | 0.024 ± 0.017 | 2.50E-15 | 3243.24 |
| PSSDR1 | Capsules | M683.2957T249 | 2 | C39H43N2O9 | | 0.0000072 ± 0.000022 | 0.022 ± 0.016 | 3.30E-11 | 3055.56 |
| PSSDR1 | Capsules | M683.2958T252 | 2 | C39H43N2O9 | | 0 ± 0 | 0.012 ± 0.0083 | 5.80E-12 | Inf |
| PSSDR1 | Capsules | M506.2156T157 | 2 | C24H32N3O9 | | 0.0000095 ± 0.000028 | 0.0093 ± 0.0069 | 2.20E-13 | 978.95 |
| PSSDR1 | Capsules | M179.0701T82 | 1 | C10H11O3 | | 0.00002 ± 0.00004 | 0.0084 ± 0.0081 | 8.00E-06 | 420.00 |
| PSSDR1 | Capsules | M575.2734T182 | 2 | C45H35 | | 0.000011 ± 0.000032 | 0.0049 ± 0.0043 | 2.60E-07 | 445.45 |
| PSSDR1 | Capsules | M416.1696T181 | 1 | C22H26NO7 | Narcotinehemiacetal (putative) | 0 ± 0 | 0.0042 ± 0.0054 | 3.30E-04 | Inf |

| | | | | | | | | | |
|---|---|---|---|---|---|---|---|---|---|
| PSSDR1 | Capsules | M494.2160T140 | 2 | C28H32NO7 | | 0 ± 0 | 0.0039 ± 0.0034 | 3.90E-09 | Inf |
| PSSDR1 | Capsules | M815.3520T236 | 2 | C48H51N2O10 | | 0 ± 0 | 0.0018 ± 0.0019 | 1.60E-07 | Inf |
| PSSDR1 | Latex | M416.1680T215 | 1 | C17H26N3O9 | Narcotinehemiacetal (putative) | 0.0036 ± 0.0048 | 5 ± 3.8 | 8.90E-08 | 1388.89 |
| PSSDR1 | Latex | M220.0963T91 | 1 | C12H14NO3 | | 0.000031 ± 0.000094 | 0.04 ± 0.029 | 2.30E-06 | 1290.32 |
| PSSDR1 | Latex | M683.2952T255 | 2 | C39H43N2O9 | | 0 ± 0 | 0.0099 ± 0.0092 | 1.60E-03 | Inf |
| PSSDR1 | Latex | M506.2151T202 | 1 | C24H32N3O9 | | 0 ± 0 | 0.0081 ± 0.011 | 1.80E-02 | Inf |
| PSMT2 | Capsules | M400.1403T124 | 1 | C21H22NO7 | Narcotoline | 1.3 ± 0.42 | 12 ± 6.7 | 3.40E-09 | 9.23 |
| PSMT2 | Capsules | M562.1937T125 | 2 | C15H36N3O19 | | 0.018 ± 0.01 | 0.32 ± 0.51 | 8.90E-03 | 17.78 |
| PSMT2 | Capsules | M442.1512T161 | 2 | C11H28N3O15 | | 0.017 ± 0.011 | 0.24 ± 0.19 | 1.80E-07 | 14.12 |
| PSMT2 | Capsules | M683.2626T150 | 2 | C43H39O8 | | 0.011 ± 0.003 | 0.11 ± 0.055 | 3.90E-09 | 10.00 |
| PSMT2 | Capsules | M195.0659T151 | 1 | C10H11O4 | | 0.031 ± 0.0037 | 0.1 ± 0.036 | 7.00E-09 | 3.23 |
| PSMT2 | Capsules | M460.1614T72 | 1 | C23H26NO9 | | 0.012 ± 0.0046 | 0.074 ± 0.051 | 1.20E-07 | 6.17 |
| PSMT2 | Capsules | M825.3442T124 | 1 | C42H53N2O15 | | 0.007 ± 0.0053 | 0.063 ± 0.053 | 3.80E-05 | 9.00 |
| PSMT2 | Capsules | M418.1507T67 | 1 | C21H24NO8 | | 0.0044 ± 0.0018 | 0.043 ± 0.023 | 2.90E-09 | 9.77 |
| PSMT2 | Capsules | M256.0605T79 | 1 | C14H10NO4 | | 0.0012 ± 0.0013 | 0.033 ± 0.015 | 3.40E-06 | 27.50 |
| PSMT2 | Capsules | M400.1402T72 | 1 | C21H22NO7 | | 0.0047 ± 0.002 | 0.031 ± 0.025 | 8.20E-06 | 6.60 |
| PSMT2 | Capsules | M400.1403T67 | 1 | C21H22NO7 | | 0.0028 ± 0.001 | 0.03 ± 0.02 | 9.50E-08 | 10.71 |
| PSMT2 | Capsules | M414.1563T155 | 1 | C22H24NO7 | | 0.006 ± 0.0032 | 0.028 ± 0.02 | 7.40E-05 | 4.67 |
| PSMT2 | Capsules | M212.0926T92 | 1 | C10H14NO4 | | 0.0085 ± 0.0018 | 0.018 ± 0.0048 | 4.70E-04 | 2.12 |
| PSMT2 | Capsules | M460.1984T210 | 1 | C24H30NO8 | Papaveroxinoline (putative) | 0.0039 ± 0.00092 | 0.017 ± 0.0066 | 3.50E-09 | 4.36 |
| PSMT2 | Capsules | M446.1825T138 | 1 | C23H28NO8 | | 0.000056 ± 0.000065 | 0.015 ± 0.013 | 3.70E-07 | 267.86 |
| PSMT2 | Capsules | M416.1356T67 | 1 | C21H22NO8 | | 0.0019 ± 0.0014 | 0.012 ± 0.017 | 2.50E-04 | 6.32 |
| PSMT2 | Capsules | M208.0976T78 | 1 | C11H14NO3 | | 0.0025 ± 0.00068 | 0.011 ± 0.007 | 1.00E-06 | 4.40 |
| PSMT2 | Capsules | M354.1350T155 | 1 | C20H20NO5 | Protopine (putative) | 0.0015 ± 0.0013 | 0.0098 ± 0.0081 | 1.40E-04 | 6.53 |
| PSMT2 | Capsules | M182.0818T36 | 1 | C9H12NO3 | | 0.0026 ± 0.0013 | 0.0089 ± 0.0051 | 4.80E-03 | 3.42 |
| PSMT2 | Capsules | M402.1560T132 | 1 | C21H24NO7 | | 0.00045 ± 0.00068 | 0.0074 ± 0.011 | 2.90E-02 | 16.44 |
| PSMT2 | Capsules | M272.0554T75 | 1 | C14H10NO5 | | 0.00014 ± 0.00018 | 0.0053 ± 0.0029 | 1.90E-04 | 37.86 |
| PSMT2 | Capsules | M444.1672T168 | 1 | C23H26NO8 | | 0.000063 ± 0.00013 | 0.0032 ± 0.0047 | 8.50E-03 | 50.79 |
| PSMT2 | Capsules | M404.2078T174 | 1 | C22H30NO6 | | 0.0016 ± 0.00035 | 0.0028 ± 0.00056 | 2.50E-14 | 1.75 |
| PSMT2 | Capsules | M491.2191T135 | 1 | C28H31N2O6 | | 0.000052 ± 0.000097 | 0.0024 ± 0.0037 | 8.40E-04 | 46.15 |
| PSMT2 | Capsules | M372.1446T102 | 1 | C20H22NO6 | | 0.000043 ± 0.000054 | 0.0018 ± 0.0014 | 2.60E-07 | 41.86 |
| PSMT2 | Capsules | M192.0667T59 | 1 | C10H10NO3 | | 0.00064 ± 0.0002 | 0.0017 ± 0.00073 | 6.80E-03 | 2.66 |
| PSMT2 | Capsules | M506.1817T159 | 2 | C28H28NO8 | | 0.00016 ± 0.00024 | 0.0014 ± 0.0012 | 9.70E-05 | 8.75 |

| | | | | | | | | | |
|---|---|---|---|---|---|---|---|---|---|
| PSMT2 | Capsules | M578.1883T70 | 2 | C15H36N3O20 | | 0.000032 ± 0.00007 | 0.0013 ± 0.0021 | 2.30E-02 | 40.63 |
| PSMT2 | Capsules | M334.2238T71 | 1 | C16H32NO6 | | 0.0029 ± 0.0015 | 0.001 ± 0.00051 | 5.50E-03 | 0.34 |
| PSMT2 | Capsules | M458.1465T92 | 2 | C11H28N3O16 | | 0.000072 ± 0.000083 | 0.00092 ± 0.00087 | 5.70E-06 | 12.78 |
| PSMT2 | Capsules | M386.1246T80 | 1 | C20H20NO7 | | 0.000005 ± 0.000013 | 0.00077 ± 0.00077 | 4.20E-06 | 154.00 |
| PSMT2 | Latex | M400.1405T118 | 1 | C21H22NO7 | Narcotoline | 0.53 ± 0.16 | 14 ± 5.6 | 1.60E-15 | 26.42 |
| PSMT2 | Latex | M442.1507T161 | 2 | C23H24NO8 | | 0.00095 ± 0.00089 | 0.18 ± 0.091 | 1.60E-14 | 189.47 |
| PSMT2 | Latex | M206.0819T69 | 1 | C11H12NO3 | | 0.0013 ± 0.0012 | 0.079 ± 0.034 | 5.80E-16 | 60.77 |
| PSMT2 | Latex | M223.0973T84 | 1 | C12H15O4 | | 0.073 ± 0.03 | 0.066 ± 0.021 | 4.50E-11 | 0.90 |
| PSMT2 | Latex | M683.2625T146 | 2 | C43H39O8 | | 0 ± 0 | 0.036 ± 0.023 | 1.90E-09 | Inf |
| PSMT2 | Latex | M418.1512T66 | 1 | C21H24NO8 | | 0.000031 ± 0.000099 | 0.035 ± 0.016 | 6.70E-13 | 1129.03 |
| PSMT2 | Latex | M400.1405T66 | 1 | C21H22NO7 | | 0.00022 ± 0.0003 | 0.034 ± 0.015 | 2.00E-13 | 154.55 |

**Table S8. Primer sequences and associated information** (provided as separate Excel file).

**Table S9. Text file of the 401 Kb region of genomic DNA depicted in Fig. 3 and detailed in Table S5.** Gaps representing short highly repetitive regions are denoted by a sequence of 100 Ns and are detailed further in the NCBI accessions.

## References


1. P. J. Robiquet, Observations sur le mémoire de M. Sertuerner relatif à l'analyse de l'opium. *Annales de Chimie et de Physique* **5**, 275 (1817).

2. H. Konzett, E. Rothlin, Zur Wirkung von Narkotin auf den Hustenreflex und auf die Bronchialmuskulatur [The effect of narcotine on cough reflex and on bronchial musculature]. *Experientia* **10**, 472 (1954). doi:10.1007/BF02170409 Medline

3. M. O. Karlsson, B. Dahlström, S.-Å. Eckernäs, M. Johansson, A. T. Alm, Pharmacokinetics of oral noscapine. *Eur. J. Clin. Pharmacol.* **39**, 275 (1990). doi:10.1007/BF00315110 Medline

4. K. Ye *et al*., Opium alkaloid noscapine is an antitumor agent that arrests metaphase and induces apoptosis in dividing cells. *Proc. Natl. Acad. Sci. U.S.A.* **95**, 1601 (1998). doi:10.1073/pnas.95.4.1601 Medline

5. Y. Ke *et al*., Noscapine inhibits tumor growth with little toxicity to normal tissues or inhibition of immune responses. *Cancer Immunol. Immunother.* **49**, 217 (2000). doi:10.1007/s002620000109 Medline

6. J. Zhou *et al*., Paclitaxel-resistant human ovarian cancer cells undergo c-Jun NH2-terminal kinase-mediated apoptosis in response to noscapine. *J. Biol. Chem.* **277**, 39777 (2002). doi:10.1074/jbc.M203927200 Medline

7. M. Mahmoudian, P. Rahimi-Moghaddam, The anti-cancer activity of noscapine: A review. *Recent Pat. Anti-Cancer Drug Discov.* **4**, 92 (2009). doi:10.2174/157489209787002524

8. J. W. Landen *et al*., Noscapine alters microtubule dynamics in living cells and inhibits the progression of melanoma. *Cancer Res.* **62**, 4109 (2002). Medline

9. D. G. I. Kingston, Tubulin-interactive natural products as anticancer agents. *J. Nat. Prod.* **72**, 507 (2009). doi:10.1021/np800568j Medline

10. J. Ziegler, P. J. Facchini, Alkaloid biosynthesis: Metabolism and trafficking. *Annu. Rev. Plant Biol.* **59**, 735 (2008). doi:10.1146/annurev.arplant.59.032607.092730 Medline

11. R. Lenz, M. H. Zenk, Acetyl coenzyme A:salutaridinol-7-*O*-acetyltransferase from *Papaver somniferum* plant cell cultures: The enzyme catalyzing the formation of thebaine in morphine biosynthesis. *J. Biol. Chem.* **270**, 31091 (1995). Medline

12. B. Unterlinner, R. Lenz, T. M. Kutchan, Molecular cloning and functional expression of codeinone reductase: The penultimate enzyme in morphine biosynthesis in the opium poppy *Papaver somniferum*. *Plant J.* **18**, 465 (1999). doi:10.1046/j.1365-313X.1999.00470.x Medline

13. T. Grothe, R. Lenz, T. M. Kutchan, Molecular characterization of the salutaridinol 7-*O*-acetyltransferase involved in morphine biosynthesis in opium poppy *Papaver somniferum*. *J. Biol. Chem.* **276**, 30717 (2001). doi:10.1074/jbc.M102688200 Medline

14. J. Ziegler *et al*., Comparative transcript and alkaloid profiling in *Papaver* species identifies a short chain dehydrogenase/reductase involved in morphine biosynthesis. *Plant J.* **48**, 177 (2006). doi:10.1111/j.1365-313X.2006.02860.x Medline

15. A. Gesell *et al*., CYP719B1 is salutaridine synthase, the C-C phenol-coupling enzyme of morphine biosynthesis in opium poppy. *J. Biol. Chem.* **284**, 24432 (2009). doi:10.1074/jbc.M109.033373 Medline

16. J. M. Hagel, P. J. Facchini, Dioxygenases catalyze the O-demethylation steps of morphine biosynthesis in opium poppy. *Nat. Chem. Biol.* **6**, 273 (2010). doi:10.1038/nchembio.317 Medline

17. A. R. Battersby, M. Hirst, D. J. McCaldin, R. Southgate, J. Staunton, Alkaloid biosynthesis. XII. The biosynthesis of narcotine. *J. Chem. Soc. Perkin 1* **17**, 2163 (1968).

18. See supplementary materials on *Science* Online.

19. B. Field *et al*., Formation of plant metabolic gene clusters within dynamic chromosomal regions. *Proc. Natl. Acad. Sci. U.S.A.* **108**, 16116 (2011). doi:10.1073/pnas.1109273108 Medline

20. K. Higo, Y. Ugawa, M. Iwamoto, T. Korenaga, Plant cis-acting regulatory DNA elements (PLACE) database: 1999. *Nucleic Acids Res.* **27**, 297 (1999). doi:10.1093/nar/27.1.297 Medline

21. N. R. Apuya *et al*., Enhancement of alkaloid production in opium and California poppy by transactivation using heterologous regulatory factors. *Plant Biotechnol. J.* **6**, 160 (2008). doi:10.1111/j.1467-7652.2007.00302.x Medline

22. N. Kato *et al*., Identification of a WRKY protein as a transcriptional regulator of benzylisoquinoline alkaloid biosynthesis in *Coptis japonica*. *Plant Cell Physiol.* **48**, 8 (2007). doi:10.1093/pcp/pcl041 Medline

23. L. C. Hileman, S. Drea, G. Martino, A. Litt, V. F. Irish, Virus-induced gene silencing is an effective tool for assaying gene function in the basal eudicot species *Papaver somniferum* (opium poppy). *Plant J.* **44**, 334 (2005). doi:10.1111/j.1365-313X.2005.02520.x Medline

24. N. Takeshita *et al*., Molecular cloning and characterization of S-adenosyl-L-methionine:scoulerine-9-*O*-methyltransferase from cultured cells of *Coptis japonica*. *Plant Cell Physiol.* **36**, 29 (1995). Medline

25. M. L. Díaz Chávez, M. Rolf, A. Gesell, T. M. Kutchan, Characterization of two methylenedioxy bridge-forming cytochrome P450-dependent enzymes of alkaloid formation in the Mexican prickly poppy *Argemone mexicana*. *Arch. Biochem. Biophys.* **507**, 186 (2011). doi:10.1016/j.abb.2010.11.016 Medline

26. N. Ikezawa, K. Iwasa, F. Sato, CYP719A subfamily of cytochrome P450 oxygenases and isoquinoline alkaloid biosynthesis in *Eschscholzia californica*. *Plant Cell Rep.* **28**, 123 (2009). doi:10.1007/s00299-008-0624-8 Medline

27. D. K. Liscombe, P. J. Facchini, Molecular cloning and characterization of tetrahydroprotoberberine *cis*-*N*-methyltransferase, an enzyme involved in alkaloid biosynthesis in opium poppy. *J. Biol. Chem.* **282**, 14741 (2007). doi:10.1074/jbc.M611908200 Medline

28. A. M. Takos *et al*., Genomic clustering of cyanogenic glucoside biosynthetic genes aids their identification in *Lotus japonicus* and suggests the repeated evolution of this chemical

defence pathway. *Plant J.* **68**, 273 (2011). doi:10.1111/j.1365-313X.2011.04685.x Medline

29. B. Field, A. E. Osbourn, Metabolic diversification—independent assembly of operon-like gene clusters in different plants. *Science* **320**, 543 (2008). doi:10.1126/science.1154990 Medline

30. M. Frey *et al*., Analysis of a chemical plant defense mechanism in grasses. *Science* **277**, 696 (1997). doi:10.1126/science.277.5326.696 Medline

31. S. Swaminathan, D. Morrone, Q. Wang, D. B. Fulton, R. J. Peters, CYP76M7 is an *ent*-cassadiene C11α-hydroxylase defining a second multifunctional diterpenoid biosynthetic gene cluster in rice. *Plant Cell* **21**, 3315 (2009). doi:10.1105/tpc.108.063677 Medline

32. H.-Y. Chu, E. Wegel, A. Osbourn, From hormones to secondary metabolism: The emergence of metabolic gene clusters in plants. *Plant J.* **66**, 66 (2011). doi:10.1111/j.1365-313X.2011.04503.x Medline

33. S. Chang, J. Puryear, J. Cairney, A simple and efficient method for isolating RNA from pine trees. *Plant Mol. Biol. Rep.* **11**, 113 (1993). doi:10.1007/BF02670468

34. M. Meyer, U. Stenzel, M. Hofreiter, Parallel tagged sequencing on the 454 platform. *Nat. Protoc.* **3**, 267 (2008). doi:10.1038/nprot.2007.520 Medline

35. X. Huang, A. Madan, CAP3: A DNA sequence assembly program. *Genome Res.* **9**, 868 (1999). doi:10.1101/gr.9.9.868 Medline

36. S. F. Altschul *et al*., Gapped BLAST and PSI-BLAST: A new generation of protein database search programs. *Nucleic Acids Res.* **25**, 3389 (1997). doi:10.1093/nar/25.17.3389 Medline

37. C. A. Smith, E. J. Want, G. O'Maille, R. Abagyan, G. Siuzdak, XCMS: Processing mass spectrometry data for metabolite profiling using nonlinear peak alignment, matching, and identification. *Anal. Chem.* **78**, 779 (2006). doi:10.1021/ac051437y Medline

38. R. Tautenhahn, C. Böttcher, S. Neumann, Highly sensitive feature detection for high resolution LC/MS. *BMC Bioinformatics* **9**, 504 (2008). doi:10.1186/1471-2105-9-504 Medline

39. C. Kuhl, R. Tautenhahn, C. Böttcher, T. R. Larson, S. Neumann, CAMERA: An integrated strategy for compound spectra extraction and annotation of liquid chromatography/mass spectrometry data sets. *Anal. Chem.* **84**, 283 (2012). doi:10.1021/ac202450g Medline

40. Q. Tao, A. Wang, H. B. Zhang, One large-insert plant-transformation-competent BIBAC library and three BAC libraries of Japonica rice for genome research in rice and other grasses. *Theor. Appl. Genet.* **105**, 1058 (2002). doi:10.1007/s00122-002-1057-3 Medline

41. J. Sambrook, D. Russell, *Molecular Cloning, A Laboratory Manual* (Cold Spring Harbor Laboratory Press, New York, ed. 3, 2001), vol. 1, chap. 1.

42. A. A. Salamov, V. V. Solovyev, Ab initio gene finding in *Drosophila* genomic DNA. *Genome Res.* **10**, 516 (2000). doi:10.1101/gr.10.4.516 Medline

43. J. D. Thompson, D. G. Higgins, T. J. Gibson, CLUSTAL W: Improving the sensitivity of progressive multiple sequence alignment through sequence weighting, position-specific

gap penalties and weight matrix choice. *Nucleic Acids Res.* **22**, 4673 (1994). doi:10.1093/nar/22.22.4673 Medline

44. Y. Liu, M. Schiff, R. Marathe, S. P. Dinesh-Kumar, Tobacco *Rar1*, *EDS1* and *NPR1/NIM1* like genes are required for N-mediated resistance to tobacco mosaic virus. *Plant J.* **30**, 415 (2002). doi:10.1046/j.1365-313X.2002.01297.x Medline

45. F. Ratcliff, A. M. Martin-Hernandez, D. C. Baulcombe, Tobacco rattle virus as a vector for analysis of gene function by silencing. *Plant J.* **25**, 237 (2001). doi:10.1046/j.0960-7412.2000.00942.x Medline

46. K. J. Livak, T. D. Schmittgen, Analysis of relative gene expression data using real-time quantitative PCR and the $2^{(-\Delta\Delta C(T))}$ method. *Methods* **25**, 402 (2001). doi:10.1006/meth.2001.1262 Medline

47. K. M. Hawkins, C. D. Smolke, Production of benzylisoquinoline alkaloids in *Saccharomyces cerevisiae*. *Nat. Chem. Biol.* **4**, 564 (2008). doi:10.1038/nchembio.105 Medline

48. G. Sariyar, Biodiversity in the alkaloids of Turkish *Papaver* species. *Pure Appl. Chem.* **74**, 557 (2002). doi:10.1351/pac200274040557